NON-BOILING HEAT TRANSFER IN DOWNWARD INCLINED GAS-LIQUID TWO PHASE FLOW

By

TAREBI JOSEPH JOHN

Bachelor of Science in Mechanical Engineering

Midwestern State University

Wichita Falls, Texas

2013

Submitted to the Faculty of the
Graduate College of the
Oklahoma State University
in partial fulfillment of
the requirements for
the Degree of
MASTER OF SCIENCE
July, 2015

NON-BOILING HEAT TRANSFER IN

DOWNWARD INCLINED GAS-LIQUID TWO PHASE

FLOW

Thesis Approved:

Dr. Afshin Ghajar

Thesis Adviser

Dr. Khaled A. Sallam

Dr. AJ Johannes

ACKNOWLEDGEMENTS

I would like to thank the people that have been instrumental in completing my master's degree. I would not have made it this far without the continuous mentoring, support, and guidance from these people.

Firstly, I want to extend my gratitude to Dr. Afshin J. Ghajar for giving me this great opportunity to be part of his research group. Your guidance throughout my master's program has helped me become a better student, researcher, and person. I would also like to extend my deep gratitude to Dr. Khaled A. Sallam and Dr. AJ Johannes for their supportive roles as committee members.

Secondly, I would like to thank Swanand Bhagwat, Srinaga Kalapatapu, Edgar Barboza, and Tabassum Hossainy for all the training they have provided me. They have done a good job in showing me the ins and outs of how to operate the experimental setup. Also, I want to thank my lab partner, Ranga Korivi, for his enormous help. His is definitely a great team member.

Finally, all these accomplishments would not have been possible without the immense support from my family. I would not have made it this far without their moral, financial, and spiritual support. I want to thank my mother, Mrs. Rose John, for all the love she has showered on me. You are the best mother any child could ask for. I am grateful to my father, Mr. John Osuoku, for his patience, kindness, and unwavering love. Also, I want to thank by siblings, Oyinkro John, Enebi John, and Deseiye John for their support.

Name: JOHN, TAREBI JOSEPH

Date of Degree: JULY, 2015

Title of Study: NON-BOILING HEAT TRANSFER IN DOWNWARD INCLINED GAS-LIQUID TWO PHASE FLOW

Major Field: MECHANICAL AND AEROSPACE ENGINEERING

Abstract: Non-boiling heat transfer in downward inclined gas-liquid two phase flow is quite intriguing and is one of the least studied phenomenon in the two phase flow literature. To explore and understand this phenomenon, experiments are carried out to measure the local and averaged non-boiling two phase heat transfer coefficient (h_{TP}) in 0, -5, -10, -20, -30, -45, -60, -75 and -90 degrees of pipe inclinations. The experiments are carried out with uniform wall heat flux boundary condition in 12.5 mm I.D. stainless steel pipe that uses air-water as fluid combination and consists of all flow patterns that covers the gas and liquid superficial Reynolds numbers in a range of 270 to 19000 and 2300 to 17000, respectively. It is observed that an increase in downward pipe inclination from horizontal initially exhibits a decreasing tendency of h_{TP} till -30 degrees and thereafter increases consistently with further increase in the pipe inclination towards vertical downward direction. The general trends of two phase heat transfer coefficients are found to be closely related to the physical structure of the flow patterns and their morphological variations as a function of pipe orientation and phase flow rates. The measured data is compared against some of the relevant non-boiling two phase heat transfer correlations available in the two phase flow literature. Based on this statistical comparison, the relatively top performing correlation is identified and proposal of an improved correlation is presented.

TABLE OF CONTENTS

LIST OF TABLES

Table Page

LIST OF FIGURES

Figure Page

NOMENCLACURE

A	cross sectional area, m^2
c	specific heat capacity, kJ/kg.K
D_i	inside diameter of pipe, m
D_o	outside diameter of pipe, m
f	function operator, dimensionless
F_p	flow pattern factor, dimensionless
F_s	shape factor, dimensionless
G	mass flux, kg/m²s
Gr	Grashof number, dimensionless
g	gravitational acceleration, m/s^2
I	electric current, A or inclination factor, dimensionless from Tang and Ghajar (2007)
h	heat transfer coefficient, W/m².K
$\bar{h}$	local average heat transfer coefficient, W/m².K
k	thermal conductivity, W/m.K
K	slip ratio, dimensionless
l	length of test section, m

$\dot{m}$	mass flow rate, kg/s
Nu	Nusselt number (= hD_i/k), dimensionless
N	number of data points, dimensionless
N_{ST}	number of thermocouple stations, dimensionless
Pr	Prandtl number (= $c\mu/k$), dimensionless
p	pressure, Pa
p_a	atmospheric pressure, Pa
p_{sys}	system pressure, Pa
$\dot{q}$	heat transfer rate, W
$\dot{q}''$	heat flux, W/m^2
R	electrical resistance, Ω
R_L	liquid hold up, dimensionless
R_t	thermal resistance, m^{2}K/W
R_v	gas to liquid volumetric ratio, dimensionless
Re	Reynolds number (= $\rho VD_i/\mu$), dimensionless
T	temperature, ^{o}C
$\bar{T}$	average temperature, ^{o}C
V	average velocity, m/s
V_D	voltage drop, V

w uncertainty, dimension varies with measured parameter

x flow quality $\dot{m}_G/\dot{m}$, dimensionless

x_n independent variable, dimension varies with variable

z axial direction, m

Greek Symbols

α void fraction, dimensionless

Δ differential operator, dimensionless

ε error, dimensionless

$\bar{\varepsilon}$ mean error, dimensionless

μ dynamic viscosity, N.m/s^2

v kinematic viscosity, m^2/s

ρ density, kg/m^3

σ surface tension, N/m

θ inclination angle of pipe or test section, deg. or rad.

Subscripts

b bulk

cal calculated

exp experimental

G gas phase

H homogeneous mixture

in inlet

j index in the circumferential direction, or *j*th component of data set

L liquid phase

m mixture

n number of variable

out outlet

SG superficial gas

SL superficial liquid

TP two phase

w wall

wi inner wall

wo outer wall

Superscripts

p constant exponent, dimensionless

CHAPTER I

INTRODUCTION

Multiphase flow is a flow that comprises of more than one phase. This can be broadly classified as either two or three phase flow. Two phase flow is a type of multiphase flow that involves only two phases such as gas-liquid, gas-solid or liquid-solid flow. This study focuses primarily on two phase gas-liquid flow. Understanding the physics that governs two phase flow is paramount since two phase flow occurs in numerous industrial processes and engineering applications. Researchers in the area of two phase flow have continued to encounter immense difficulty in trying to completely model two phase flow. This difficulty is partly due to the fact that there are interfacial interactions between the two phases and providing the appropriate boundary conditions makes it extremely difficult to provide a closed form solution to Navier-Stokes equation. This is one of the reasons why both the theoretical and computational approach in understanding two phase flow is extremely difficult. The ability to describe two phase flow through these methods diminishes when turbulence is introduced to the flow. In this study, an experimental approach has been employed to describe the heat transfer physics of two phase flow. This method is appropriate as long as the laboratory model can be extrapolated to a full scale scenario using computational or theoretical approach.

It is important to highlight the immense importance of two phase flow. During the production of two phase hydrocarbon fluids from oil reservoirs and its transportation to the surface processing facilities, the temperature of hydrocarbons drops drastically and is favorable for hydrates formation and wax deposition. Wax deposition can result in problems including reduction of inner tube diameter causing blockage, increased surface roughness of tube leading to restricted flow line pressure, decrease in production, and various mechanical problems. In such situations, the proper knowledge of heat transfer coefficient in non-boiling two phase flow is crucial for the purpose of flow assurance in oil and gas industry.

Another important application is in the power station where boilers are used to produce superheated steam from pressurized water by heating through pipes. The steam is used for running the turbines which are used to produce electricity. Designing such equipment requires detailed understanding and knowledge of heat transfer and pressure drop in two phase flow to ensure appropriate supply and regulation of the generated steam to the turbine. Other industrial application of two phase flow can be found in condensation of refrigerant used in air conditioning, heat pump systems, chemical and petro chemical process, and nuclear reactors. This means that a good understanding of the heat transfer dynamics in two phase flow is beneficial in a wide range of industrial applications.

Due to the immense importance of two phase flow outlined above, various research have been conducted in non-boiling two phase heat transfer for inclined pipes. Some of the experimental and modelling work in the field of non-boiling two phase heat transfer in downward inclined systems are those of Chu and Jones (1980), Oshinowo et al. (1984), Bhagwat et al. (2012) and Hossainy et al. (2014). Chu and Jones (1980) measured two phase heat transfer coefficient in vertical upward and downward pipe inclinations using air-water as working fluids. They found out that in comparison to vertical downward flow, two phase heat transfer coefficients in vertical

upward flow were substantially higher particularly in the intermittent and annular flow regime. Similarly, Oshinowo et al. (1984) conducted research for both upward and downward flows. Their experiments were done in a 25.8 mm I.D. with air-water mixture. They also observed that heat transfer coefficients were higher for upward flow as compared to downward flow. They noted that the effect of inclination was more pronounced at low liquid flow rates. Bhagwat et al. (2012) also studied heat transfer coefficient in vertical downward air-water two phase flow. Their work was focused on the effect of flow patterns on two phase heat transfer coefficient. They noted that heat transfer for two phase flow was much higher than that of single phase flow especially in the annular flow regime. One of the most recent and only work found in the literature that addresses the effect of pipe inclination for horizontal and near horizontal downward two phase flow on two phase heat transfer coefficient (h_{TP}) is the work of Hossainy et al. (2014). Experimental measurements were carried out in a 12.5 mm I.D. schedule for air-water mixture for $0^o \leq \theta \leq -20^o$ pipe inclinations. They noted in their work a significant decrease in heat transfer coefficient as the pipe was inclined from 0^o to -20^o. As seen above, nothing in the literature addresses the effect of pipe inclination as the pipe is inclined from 0^o to -90^o. This is why this work is extremely important since it addresses the effect of pipe inclination on two phase heat transfer coefficient in these pipe orientations ($0^o \leq \theta \leq -90^o$). The results obtained from this work will be beneficial in providing closure to non-boiling heat transfer coefficient trend in downward pipe inclination. Also, the results obtained will enable the development of a comprehensive heat transfer correlation that will be able to predict heat transfer coefficient for any downward pipe orientation, flow pattern, fluid combination, and pipe diameter.

1.1 Definitions and Terminologies

In this section, an overview of terminologies used to describe two phase flow is presented. These terms include mass flow rate, Reynolds number, void fraction, mass flux, superficial liquid and gas velocity, Nusselt number, and Prandtl number. It is imperative that the importance and role of

these terms are fully understood so as to facilitate the comprehension of two phase flow physics as it applies to this work.

Two phase mass flow rate is the summation of the gas and liquid mass flow rates.

$$\dot{m} = \dot{m}_G + \dot{m}_L \tag{1.1}$$

The definition of liquid, gas and mixture mass flux are as follows:

$$G_G = \frac{\dot{m}_G}{A} \tag{1.2a}$$

$$G_L = \frac{\dot{m}_L}{A} \tag{1.2b}$$

$$G = \frac{\dot{m}}{A} \tag{1.2c}$$

Cross sectional area is the summation of the cross sectional area occupied by both the liquid and gas phase.

$$A = A_G + A_L \tag{1.3}$$

The quality of the flow shows the ratio of mass flux of gas to that of the total mass flow rate of the mixture.

$$x = \frac{\dot{m}_G}{\dot{m}} \tag{1.4}$$

The void fraction is the ratio of the cross-sectional area occupied by the gas phase to that of the entire cross section as shown below.

$$\alpha = \frac{A_G}{A} \tag{1.5}$$

The liquid hold up is defined as:

$$R_L = 1-\alpha = \frac{A_L}{A} \tag{1.6}$$

Mixture density is defined as follows:

$$\rho_m = \alpha\rho_G + (1-\alpha)\rho_L \tag{1.7}$$

The mixture density for homogenous mixture is defined as:

$$\rho_H = \frac{1}{x/\rho_G + (1-x)/\rho_L} \tag{1.8}$$

Superficial gas and liquid velocity is defined as following:

$$V_{SG} = \frac{x\dot{m}}{A\rho_L} \tag{1.9}$$

$$V_{SL} = \frac{(1-x)\dot{m}}{A_L} \tag{1.10}$$

Slip ratio is the relative velocity of the gas phase with respect to the liquid phase.

$$K = \frac{V_G}{V_L} \tag{1.11}$$

Superficial gas and liquid Reynolds number are defined in terms of gas and liquid density, viscosity and superficial gas and liquid velocity as follows:

$$\mathrm{Re}_{SG} = \frac{\rho_G \mathrm{D_i} V_{SG}}{\mu_G} \tag{1.12}$$

$$\mathrm{Re}_{SL} = \frac{\rho_L \mathrm{D_i} V_{SL}}{\mu_L} \tag{1.13}$$

Some of the relevant dimensionless numbers for heat transfer analysis are Nusselt number and Prandtl number. Nusselt number is the ratio of convective to conductive heat transfer given as:

$$Nu = \frac{h\mathrm{D_i}}{k} \tag{1.14}$$

Prandtl number is the ratio of the momentum diffusivity to thermal diffusivity given as:

$$\mathrm{Pr} = \frac{\mu c}{k} \tag{1.15}$$

1.2 Flow Patterns

Understanding the visual distribution of liquid and gas phase in a two phase flow is very important in understanding the heat transfer dynamics in such flow. In this section, the flow patterns and maps for $0^o \leq \theta \leq -90^o$ pipe inclinations are discussed. The flow patterns and flow maps presented here are for air-water two phase flows. The main focus of this section is to identify the generally accepted flow patterns, discuss them, and identify their significance in predicting heat transfer coefficient. The major flow patterns found in the literature for $0^o \leq \theta \leq -20^o$ and $\theta = -90°$ pipe inclinations are bubbly, slug, intermittent, falling film, stratified and annular flow as shown in Figures 1.1 and 1.2, respectively.

Bubbly Flow: This flow is characterized by numerous bubbles dispersed in the liquid phase. These bubbles can vary in size depending on the liquid and gas flow rates. Godbole et al. (2011) observed the bubbly flow at low gas and high liquid flow rates. The bubbles were dispersed uniformly throughout the pipe cross-section. The bubbles had tendencies to move to the center of the tube and where referred to as coring-bubbly flow.

Slug Flow: This flow is characterized by long intermittent gas bubbles separated by liquid slugs that usually span a diameter equal to that of the pipe. Slug flow usually occurs at gas flow rates higher than that of the bubble flow. Godbole et al. (2011) observed cylindrical and bullet shaped gas bubbles called "Taylor slugs' in vertical upward flow. Crawford (1983) also observed distorted long slug at higher operating temperatures using R-113a and its vapor as the working fluid in a 0.038 m diameter round pipe. The slug appeared distorted because of the imbalance between the buoyant, drag and fluid viscous forces. This was particularly evident in vertical downward flow where the force due to buoyancy acts in the opposite direction to the mean flow.

Intermittent Flow: This flow pattern is used to describe transitional region of the flow. It is characterized by its wavy nature. Examples are slug wavy and annular wavy flow. These types of flows are shown in Figure 1.1. Slug wavy flow is developed when gas flow rate is increased in the slug flow region inducing waves on the gas-liquid interface due to shear force. A continued increase in the gas flow causes the liquid phase to form on the pipe wall leading to annular wavy flow.

Falling Film Flow: The falling film flow occurs at vertical and near vertical downward pipe orientations and is a special case of stratified flow. Unlike stratified flow, the entire pipe circumference is wetted by a thin liquid film that surrounds the central gas core.

Stratified Flow: This flow is characterized by the liquid and gas phase moving in two separate and distinct layers in the pipe. This flow pattern is observed in horizontal and near horizontal pipe inclinations as shown in Figure 1.1. It is observed that the gas phase flows on top of the liquid phase and touches the top of the pipe while the liquid phase touches the bottom of the pipe due to density difference, gravity, and buoyancy.

Annular Flow: This flow usually occurs at relatively high gas and liquid velocities. Annular flow is a very important flow pattern since it is known to enhance heat transfer. This flow is characterized as gas core surrounded by continuous liquid film adjacent to the pipe wall. For downward orientation, the liquid phase moves faster than the gas phase due to the influence of gravity and high inertia compared to the gas phase.

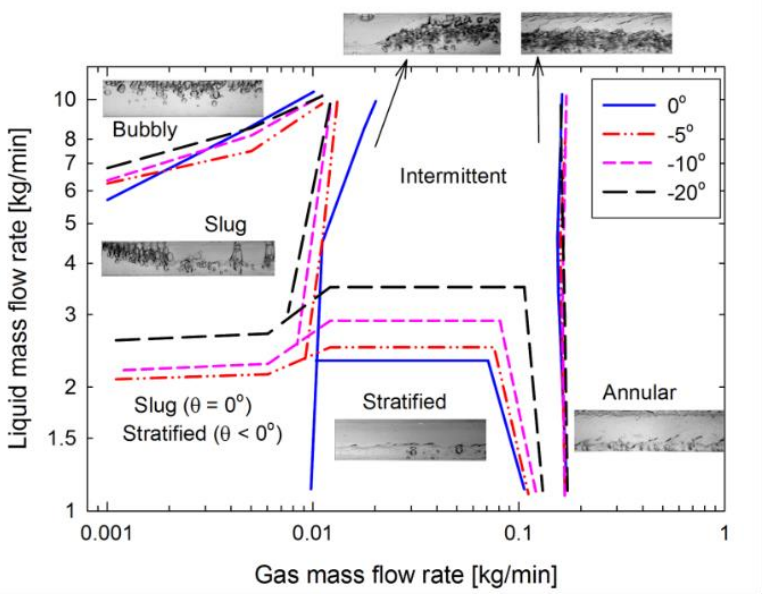

Figure 1.1 Flow map for horizontal and near horizontal downward air-water two phase flow (Hossainy et al. (2014))

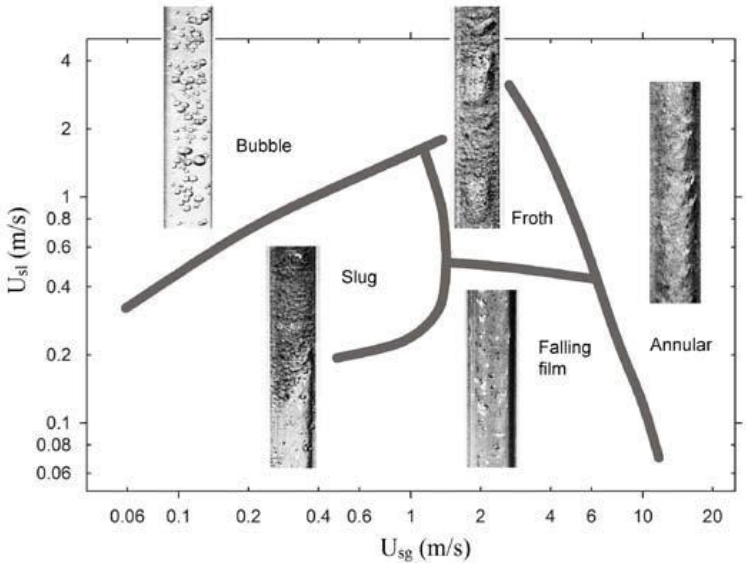

Figure 1.2 Flow map for vertical downward air-water two phase flow
(Bhagwat et al. (2012))

1.3 Research Objectives

The main objective of this research work is to investigate the effect of downward pipe inclination ($0^o \leq \theta \leq -90^o$) on heat transfer coefficient in two phase air-water mixture flow. The first part of this research will be focused on collecting experimental data in downward pipe inclination and establishing a coherent heat transfer coefficient trend as the pipe inclination is changed. After establishing a trustworthy trend, analysis of the performance of relevant heat transfer correlations as they apply to heat transfer in downward inclined air-water two phase flow will be done. A detailed study will be carried out to verify the overall performance of these correlations and recommendation for the best performing correlations will be made. After this detailed analysis, an improved correlation will be proposed. The following steps will be taken to achieve these objectives:

(1) Measurement of two phase heat transfer coefficient in downward pipe inclinations (0, -5, -10, -20, -30, -60, -75 and -90 degrees).

(2) Thorough analysis of experimental results in order to establish viable heat transfer coefficient trends.

(3) Analysis of the existing relevant heat transfer correlations for non-boiling two phase flow and recommend the best performing correlation.

(4) Propose an improved correlation based on the results obtained in step 3.

1.4 Outline

In order to achieve the research objectives outlined in the previous section, a comprehensive literature survey will be performed to discuss the relevant research works by previous authors in the field of two phase flow heat transfer. This literature survey will be documented in Chapter II titled "Literature Review." After literature survey, two phase heat transfer coefficient measurements will be done for air-water mixture. The details of the experimental setup is discussed in Chapter III titled "Experimental Setup." After collection of the data, plotting and analysis of the data points will be performed to establish the trend of heat transfer with flow patterns and pipe inclination. After establishing the trend, flow patterns and analysis of the local heat transfer coefficients will be used to provide a physical explanation of the observed trend. The experimental data will be used to test the available correlations in the literature proposed by previous authors. This test will be done for horizontal and near horizontal ($0^o \leq \theta < -30^o$), mid-range ($-30^o \leq \theta \leq -60^o$), vertical and near vertical ($60^o < \theta \leq -90^o$), and overall ($0^o \leq \theta \leq -90^o$) pipe inclinations for various flow patterns. The best performing correlation for the respective ranges of pipe orientations and various flow patterns will be identified. Based on this analysis, an improved correlation will be proposed. The analysis of the experimental data, test of correlations performance and proposal of an improved correlation will be discussed in Chapter IV tilted "Results and Discussion." Finally, in Chapter V, a summary of the research findings will be presented along with some recommendations for future work.

CHAPTER II

LITERATURE REVIEW

In this chapter, some of the works that have been done in the area of non-boiling two phase heat transfer will be addressed. This chapter is divided into two parts: "Effect of Flow Patterns and Pipe Inclination on h_{TP} (two phase heat transfer coefficient)" and "General Heat Transfer Correlations." The first section focuses on research that have been done to investigate the effect of flow patterns and pipe orientation on two phase heat transfer coefficient particularly for downward inclined pipe orientation. Research work found in the literature as discussed in this section are those of Chu and Jones (1980), Oshinowo et al. (1984), Bhagwat et al. (2012) and Hossainy et al. (2014). Overall, their work seems to suggest that there is a significant decrease in heat transfer coefficient as the pipe is inclined from vertical upward to downward pipe orientation.

The second part of this chapter addresses various general heat transfer correlations that have been proposed. Some of the work found in the literature are those of Knott et al. (1959), Aggour (1978), Chu and Jones (1980), Oshinowo et al. (1984), Shah (1981), Kim and Ghajar (2006), and Tang and Ghajar (2007). Very few researchers such as Chu and Jones (1980), Oshinowo et al. (1984), and Tang and Ghajar (2007) focused on the effect of pipe inclination on two phase heat transfer coefficient.

Tang and Ghajar (2007) took it a step further by introducing flow pattern factor (F_P) and inclination factor (I) in their proposed correlation to account for the effect of flow patterns and pipe inclination. As seen in the next sections, very limited work has been done so far to address the effect of pipe inclination on heat transfer coefficient. The only research work that addresses the effect of pipe inclination for downward orientation is the work of Hossainy et al. (2014) for $0^o \leq \theta \leq -20^o$. This is why this current research work is important as it will provide closure to the full range of downward orientations for $0^o \leq \theta \leq -90^o$

2.1 Effect of Flow Patterns and Pipe Inclination on h_{TP}

Understanding the effect of flow pattern and pipe inclination on heat transfer coefficient is very important in comprehending the heat transfer mechanism in two phase gas-liquid flow. Researchers have continued to experiment and establish viable relationship between flow pattern and variation of gas and liquid flow rates on heat transfer coefficient for different fluid combinations, pipe diameter, and pipe inclination for the past 60 years. The overall goal of performing such experiments is to enable researchers develop a robust heat transfer correlation based on the experimental data that is independent of fluid combination, pipe inclination, and other experimental conditions. Till date, such correlation does not exist. Hence, it is important that a careful analysis of the effect of flow pattern and pipe inclination on heat transfer coefficient is performed.

One of the earliest research done on heat transfer in upward and downward inclined gas-liquid two phase flow was carried out by Chu and Jones (1980). These researchers investigated the effect of flow pattern and pipe orientation on non-boiling heat transfer coefficient in air-water two phase flow. Their experimental setup consisted of a 91 cm long 2.67 cm I.D. test section with an average wall thickness of 0.32 cm. Measurements were carried out at a constant heat flux of 55 kW/m². They noted that there was an increase in h_{TP} as gas flow rate was increased for a constant

liquid flow rate. This increment was steepest for low liquid flow rate. As liquid flow rate is increased for constant gas flow rate, the slope of the heat transfer coefficient becomes less steeper. Also, Chu and Jones (1980) observed that h_{TP} for upward flow was higher than that of downward flow for the same liquid and gas flow rate. They attributed this finding to higher liquid velocity and turbulence in upward flow compared to downward flow.

Oshinowo et al. (1984) research work was concerned with the relationship of increasing gas flow rate on heat transfer coefficient in both downward and upward flow and how the heat transfer coefficients in downward flow compared with that of upward flow. Experiments were carried out in a 25.8 mm I.D. with air-water mixture in vertical pipes. The researchers plotted heat transfer coefficients against gas to liquid volumetric ratio. The authors observed a significant heat transfer enhancement as the gas to liquid volumetric ratio (R_v) increased for both upward and downward flow. Changes in the heat transfer coefficient were observed at transition boundaries particularly at the start of the froth flow where a significant increase in the heat transfer was observed. The steepest increase in the heat transfer coefficient as gas flow was increased was seen at low liquid flow rate. Also, Oshinowo et al. (1984) compared the h_{TP} for the same liquid flow rate for upward and downward flow. They observed that the heat transfer coefficient for upward flow was greater than that of downward flow. This difference was largest at high gas to liquid ratio and very low liquid flow rate where they observed as much as 70% difference. Overall, the effect of inclination on heat transfer coefficient was more pronounced at low liquid flow rates. These researchers attributed these differences in heat transfer coefficient for upward and downward flow due to difference in the flow pattern, liquid holdup, and flow structure for upward and downward flow for similar water and air flow rates.

Bhagwat et al. (2012) studied heat transfer coefficient in vertical downward air-water two phase flow. Their experiments were carried out in a 0.001252 m I.D. schedule 10 S stainless steel pipe.

The main focus of their work was to investigate the effect of flow pattern on heat transfer coefficient and compared the results of two phase and single-phase flow heat transfer coefficient. A total of 165 points were collected and the flow patterns observed were annular, slug, froth, bubbly and falling film flow. Bhagwat et al. (2012) reported that for bubbly flow, a slow but steady increase in heat transfer coefficient was observed. They noted that the heat transfer coefficient remained constant until superficial liquid Reynolds number (Re_{SL}) = 300 and started to increase as Re_{SL} exceeded 300. The researchers observed that at low and moderate superficial gas Reynolds number (Re_{SG}), the two phase heat transfer coefficient was less than that of the single-phase flow for similar Re_{SL}. At higher Re_{SG}, two phase heat transfer coefficient begins to increase and eventually surpasses that of the single-phase counterpart. One possible reason the researchers suggested to explain this trend in the bubbly region is that at low Re_{SG}, the gas bubble is forced towards the pipe axis due to buoyancy and liquid inertia which acts in the opposite direction. The concentration of the gas bubble in the pipe axis leads to an increase in the viscous sub-layer thickness which in-turn reduces the two phase heat transfer. At higher gas and liquid flow rates, the bubbles are forced to move near the pipe wall. This reduces the viscous sub-layer thickness. A reduction in the viscous sub-layer thickness increases the heat transfer coefficient for two phase flow making it greater than that of the single-phase flow counterpart. In the slug flow region, they observed a continuous increase in heat transfer coefficient with increase in gas flow rate. For higher Re_{SL}, the heat transfer coefficient was observed to be higher. They attributed this to the fact that as Re_{SL} is increased, the slug length tends to shorten hence increasing h_{TP}. This is no surprise since h_{TP} is a function of slug length and frequency. Also, for froth flow region, they observed that heat transfer coefficient for two phase flow was greater than its corresponding single-phase flow. They noted that this is due to the turbulent nature of the froth flow region which tends to enhance heat transfer. In the falling film flow region, they noted occurrence of dry spot at low gas flow rate which caused a decrease in h_{TP}, but at high gas flow rate, the liquid is forced to maintain

contact with the pipe wall thereby eliminating dry spots which leads to an increase in h_{TP}. Finally, for annular flow region, they observed an increase in h_{TP} with increasing gas flow rate similar to that reported in the froth flow region.

One of the most recent work found in the literature for horizontal and near horizontal downward two phase flow was conducted by Hossainy et al. (2014). Experimental measurements were carried out in a 12.5 mm I.D. schedule 10 S steel pipe for air-water mixture for 0, -5º, 10º, and -20º pipe inclination. As shown in Figure 2.1, Hossainy et al. (2014) observed that the heat transfer coefficient increased with increase in Re_{SL} and Re_{SG}. For similar Re_{SL} and higher Re_{SG} in the stratified region, they noted a much steeper increase of heat transfer coefficient due to much higher inertia encountered at higher Re_{SG}. Overall, Hossainy et al. (2014) highlighted that heat transfer coefficient increased in the stratified/slug flow region, remained constant in the early stages of intermittent flow, and then increased steeply as the flow approached the annular region. The researchers also noted the effect of pipe inclination on heat transfer coefficient. As shown in Figure 2.2, they found out that as the pipe was inclined from 0º to -20º, the heat transfer coefficient decreased significantly. The same trend was observed by Oshinowo et al. (1984). Hossainy et al. (2014) attributed this decrease in heat transfer coefficient due to change in the flow pattern as the pipe changed inclination from horizontal to downward horizontal inclination. They noted that as the pipe was inclined from 0º to -20º slug flow developed into stratified flow. Hence, the researchers saw a decrease of 49%, 50%, and 51% for, -5º, 10º, and -20º pipe inclination, respectively. This decrease is attributed to the fact that slug is a better conductor of heat than stratified flow due to better contact of the liquid with the top part of the pipe wall and its intermittent manner of flow. Hossainy et al. (2014) also observed that as Re_{SG} and Re_{SL} is increased or as the flow tends towards the annular region, the effect of pipe inclination becomes less pronounced as shown in Figure 2.2.

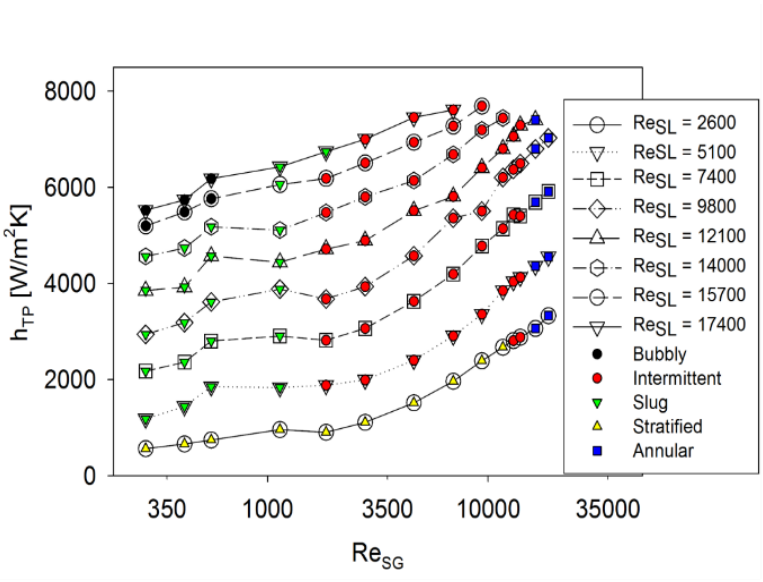

Figure 2.1 Variation of h_{TP} at a given Re_{SL} and increasing Re_{SG} for -5º (Hossainy et al. (2014))

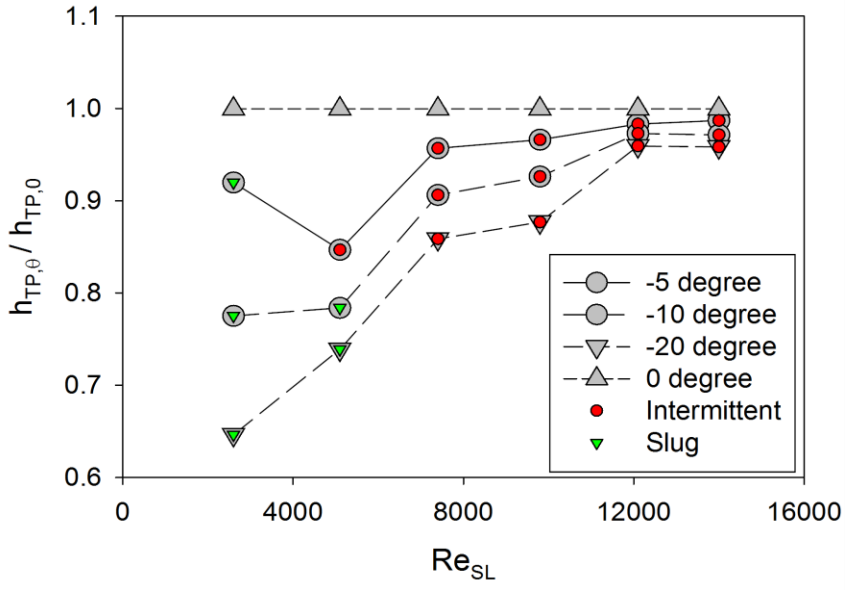

Figure 2.2 Comparison of h_{TP} at different inclinations at Re_{SG} = 4500 (Hossainy et al. (2014))

2.2 General Heat Transfer Correlations

Researchers have continued to contend with the task of developing a correlation for two phase heat transfer coefficient that is independent of pipe inclination, fluid combination, flow rate

combination, pipe diameter, and other experimental conditions. Till date, this correlation is non-existent. Due to the complexity of two phase flow, a more specific approach has been employed by researchers to predict two phase heat transfer coefficient. This approach involves collecting experimental data for specific experimental conditions (pipe diameter, fluid combination, and so on) and developing correlations to predict these set of data. This section addresses some of the prominent general heat transfer correlations found in the literature. The general correlations focuses on accounting for average mixture properties, flow rates, effect of pipe inclination, and flow patterns.

One of the earliest work on developing a general heat transfer correlation was done by Knott et al. (1959). Experiments were carried out using nitrogen-oil fluid mixture in a 304 stainless steel tube of 0.506 in. I.D. and 0.028 in. thickness. They collected ninety-three nitrogen-oil data points over a superficial liquid Reynolds number (Re_{SL}) range of 6.7 to 162 and superficial gas Reynolds number (Re_{SG}) range of 126 to 3920. They concluded from their experimental results that heat transfer coefficient in the bubbly flow region was generally higher than that of single phase flow at the same liquid flow rates because of an increase in the mean velocity when bubbles are introduced to the flow. Based on this observation, they proposed a two phase heat transfer correlation (h_{TP}) which predicted h_{TP} values slightly higher than their experimental results. The percentage of experimental data predicted by their correlation was not reported in the literature. Their proposed correlation attempted to capture the effect of injecting nitrogen on h_{TP}. The correlation is given as:

$$\frac{h_{TP}}{h_L} = (1 + \frac{V_{SG}}{V_{SL}})^{\frac{1}{3}} \tag{2.1}$$

Where h_L is calculated from Sieder and Tate (1936) as:

$$h_L = 1.86(\frac{k}{D_i})(Re_{SL}Pr_L\ \frac{D_i}{l})^{\frac{1}{3}}\left(\frac{\mu_b}{\mu_w}\right)^{0.14} \quad \text{(Laminar)} \tag{2.1a}$$

$$h_L = 0.027(\frac{k}{D_i})Re_{SL}{}^{0.8}\,Pr_L{}^{1/3}(\frac{\mu_b}{\mu_w})^{0.14} \quad \text{(Turbulent)} \tag{2.1b}$$

Dorresteijn (1970) conducted research for forced convection heat transfer for both upward and downward flow in bubbly and froth flow pattern in two phase gas-liquid mixture using oil-air as the working fluid. Electrical heating with 70 mm diameter coil was applied. The range of the liquid velocities was 0.02 to 4.64 m/s corresponding to Reynolds number range of 300 to 66,000. For liquid velocity above 1 m/s, a slight increase in the heat transfer was observed by the researchers. However, no difference in heat transfer was observed while comparing upward and downward flow. Information on how void fraction, α, was calculated was not reported in the literature. The author proposed the following correlation:

$$\frac{h_{TP}}{h_L} = (1-\alpha)^{-n} \tag{2.2}$$

Where *n* given as = 0.33 for laminar flow and 0.8 for turbulent flow. Also, h_L is given as:

$$h_L = 0.0123\, {Re_{SL}}^{0.9} {Pr_L}^{0.33} \left(\frac{\mu_b}{\mu_w}\right)^{0.14} \left(\frac{k}{D_i}\right) \tag{2.2a}$$

Martin and Sims (1971) conducted experiments in two phase flow forced convection in water with air injected in a rectangular duct consisting of a horizontal cross section with dimensions of 0.52 in. by 0.257 in. Re_{SL} and Re_{SG} ranges in which they conducted their experiments were not reported in the literature. The main dependent variables were heat transfer coefficient and flow pattern, while the independent variables were air injection and superficial velocities of gas and liquids. The proposed correlation is expressed as

$$\frac{h_{TP}}{h_L} = 1 + 0.064\left(\frac{V_{SG}}{V_{SL}}\right)^{\frac{1}{2}} \tag{2.3}$$

Where h_L is determined by Sieder and Tate (1936) equation. The authors reported that correlation predicted 88% of the measured data within range of ±20%.

Khoze et al. (1976) conducted experiments on heat transfer measurements in air-water, air-diphenyloxide, and air-polymethylsiloxane mixture flowing through rectangular channels. They carried their experiments in Re_{SG} range of 4000 to 37,000 and Re_{SL} range of 3.5 to 210. Based on the results obtained from their experiments, they proposed the following correlation:

$$Nu_{TP} = 0.26\ Re_{SG}^{0.2} Re_{SL}^{0.55} Pr_L^{0.4} \quad (2.4)$$

The correlation predicted 100% of data points within ±20% error bands.

Aggour (1978) performed measurements of two phase heat transfer coefficient for vertical upward flow for three different fluid combinations: water-air, water- helium and water-Freon 12. The tube was 1.168 cm in internal diameter and the electrically heated test section had l/D_i ratio of 130. They carried their experiments in Re_{SL} range of 4000 to 126,000 and Re_{SG} range of 20 to 13,000 for water-helium mixture and Re_{SL} range of 4000 to 56,000 and Re_{SG} range of 800 to 209,000 for water-Freon 12 mixture. The author reported that the effect of gas-phase density on heat transfer was found to be more pronounced in low liquid flow rates and moderate to high superficial gas velocities. A simple correlation was proposed which is:

$$\frac{h_{TP}}{h_L} = (1-\alpha)^{-n} \quad (2.5)$$

The correlation predicted 91% of the 338 data points within ±50%. Where n is 0.33 for laminar flow and 0.83 for turbulent flow. Void fraction (α) is calculated from Chisholm (1973). Single phase heat transfer coefficient and void fraction correlation of Chisholm (1973) are given as follows:

$$h_L = 1.615\ (\frac{k}{D_i})(Re_{SL} Pr_L \frac{D_i}{l})^{\frac{1}{3}} (\frac{\mu_b}{\mu_w})^{0.14} \quad \text{(Laminar) (2.5a)}$$

$$h_L = 0.0155 (\frac{k}{D_i}) Re_{SL}^{0.83} Pr_L^{0.5} (\frac{\mu_b}{\mu_w})^{0.33} \quad \text{(Turbulent) (2.5b)}$$

$$\alpha = [1 + (\frac{\rho_L}{\rho_m})^{1/2} \left(\frac{1-x}{x}\right) (\frac{\rho_G}{\rho_L})\ ]^{-1} \quad (2.5c)$$

Where homogenous mixture density (ρ_m) is given as:

$$\frac{1}{\rho_m} = \left(\frac{1-x}{\rho_L}\right) + (\frac{x}{\rho_G}) \quad (2.5d)$$

Ravipudi and Godbold (1978) performed measurements of two phase heat transfer coefficient in vertical steam condenser with four different liquid-gas combinations (air-water, air-toluene, air-benzene, and air-methanol) and Re_{SL} and Re_{SG} ranges of 8500 to 90,000 and 3500 to 82,000, respectively. The effect of mass transfer on heat transfer rates was investigated and for such case the heat transfer coefficients were found to be a function of liquid and gas mass flux densities, vapor pressure of the liquid, and the total pressure of the system. Based on their results, a correlation was proposed for predicting heat transfer coefficient which is given as:

$$h_{TP} = 0.56\left(\frac{k}{D}\right)Re_{SL}^{0.6}Pr_L^{0.33}\left(\frac{\mu_b}{\mu_w}\right)^{0.14}\left(\frac{\mu_b}{\mu_G}\right)^{0.2}\left(\frac{V_{SG}}{V_{SL}}\right)^{0.3} \quad (2.6)$$

The exact percentage of data points that fell within ±20% and ±30% error bands was not reported in the literature.

Chu and Jones (1980) were one of the first researchers to develop a general heat transfer correlation strictly for vertical downward two phase flow. Their experimental setup consisted of a 91 cm long 2.67 cm I.D. test section with an average wall thickness of 0.32 cm. Measurements were carried out at a constant heat flux of 55 kW/m². They conducted experiments in Re_{SL} and Re_{SG} ranges of 16000 to 112,000 and 540 to 2700, respectively. The authors included the ratio of atmospheric pressure to system pressure to account for pressure change in the system. They found the proposed correlation to predict their experimental data within ±15%. The correlation proposed for vertical downward flow is given as:

$$h_{TP} = 0.47\left(\frac{k}{D_i}\right)Re_{SL}^{0.55}Pr_L^{0.33}\left(\frac{\mu_b}{\mu_w}\right)^{0.14}\left(\frac{Pa}{P}\right)^{0.17} \quad (2.7)$$

Shah (1981) conducted experimental measurements for gas-liquid two phase flow and proposed a general correlation based on the results obtained. Their correlation was tested against several experimental data base which included: air-water, oil, nitrogen, and glycol. He reported that his

correlation predicted 96% of the data points within ±30% for Re_{SL} < 170. The proposed correlation is given as:

$$\frac{h_{TP}}{h_L} = (1 + \frac{V_{SG}}{V_{SL}})^{\frac{1}{4}} \tag{2.8}$$

Where h_L is calculated from Sieder and Tate (1936). For Re_{SL} > 170, the author presented a graphical correlation due to the complex nature of the relationship between the parameters.

Drucker et al. (1984) conducted experiments on two phase heat transfer for vertical air-water flow inside tube and over rod bundles with blockage. For air-water flow inside tube, liquid Reynolds number range was 2000 to 150,000 and void fraction was varied between 0.01 and 0.40. The following correlation was proposed:

$$\frac{h_{TP}}{h_L} = 1 + 2.5\,(\frac{\alpha Gr}{{Re_{TP}}^2})^{0.5} \tag{2.9}$$

$$\text{Where, } Gr = \frac{(\rho_L - \rho_G) g {D_i}^3}{\rho_L {\nu_L}^2} \tag{2.9a}$$

and h_L is from Sieder and Tate (1936). The authors reported that the correlation predicted most of their data within ±35%. The exact percentage of data that fell within ±35% was not reported in the literature.

Oshinowo et al. (1984) carried out experiments in a 25.8 mm I.D. with air-water mixture in vertical pipes. The gas to liquid volumetric ratio (R_v) was varied from 2 to 220 and the superficial liquid Reynolds number was varied from 1700 to 5600. The authors found out that their proposed correlation predicted their data for $1 < R_v < 250$ within ±18%. Except for a single point $R_v = 2.1$. As mentioned in the previous section, these authors observed that the heat transfer coefficient for upward flow was greater than that of downward flow. For downward flow, the correlation proposed is given as:

$$h_{TP} = 1.2(\frac{\mathrm{k}}{D_i}){Re_{SL}}^{0.6}{Pr_L}^{1/3}(\frac{\mu_b}{\mu_w})^{0.14}(\frac{\mu_G}{\mu_L})^{0.2}(\frac{V_{SG}}{V_{SL}})^{0.1} \tag{2.10}$$

Rezkallah and Sims (1987) evaluated eleven existing vertical two phase flow heat transfer correlations using selected data sets collected from the literature with thirteen different gas liquid combinations with varying pipe dimensions and flow patterns. They carried out their experiments in Re_{SL} and Re_{SG} ranges of 8300 to 21,000 and 50 to 42,000, respectively. The authors reported good agreement for most of the correlations for air-water data. The authors proposed the following correlation:

$$\frac{h_{TP}}{h_L} = (1-\alpha)^{-0.9} \tag{2.11}$$

where, h_L is from Sieder and Tate (1936) and information of how α is calculated was not provided.

Kim and Ghajar (2006) developed a correlation based on 408 experimental data points covering different flow patterns, flow combinations and pipe orientations 0°, 2°, 5°, and 7°. They carried out experiments in Re_{SL} and Re_{SG} ranges of 820 to 26,000 and 560 to 48,000, respectively. To account for the flow pattern, the authors introduced flow pattern factor (F_P). This correlation successfully predicted 93% of the data within ±20% agreement. The correlation given by the authors is

$$h_{TP} = h_L \times F_p\left(1+0.7\left[\left(\frac{x}{1-x}\right)^{0.08}\left(\frac{1-F_p}{F_p}\right)^{0.06}\left(\frac{\mathrm{Pr}_G}{\mathrm{Pr}_L}\right)^{0.03}\left(\frac{\mu_G}{\mu_L}\right)^{-0.14}\right]\right) \tag{2.12}$$

Where h_L is determined by Sieder and Tate (1936) equation, α is calculated from Chisholm (1973) given in equation (2.5c), and F_p is calculated as follows:

$$F_P = (1-\alpha) + \alpha[\frac{2}{\pi}(\tan^{-1}\sqrt{(\frac{\rho_G (V_G - V_L)^2}{gD_i(\rho_L-\rho_G)})}]^2 \tag{2.12a}$$

Tang and Ghajar (2007) are among some of the few researchers that accounted for the effect of pipe inclination (I) and flow pattern (F_p) in their proposed correlation. They performed experiments in air-water two phase flow for horizontal and near horizontal inclination in 1 in. I.D. pipe for 0º, 2º, 5º and 7º. They carried out experiments in Re_{SL} and Re_{SG} ranges of 740 to 26,000

and 560 to 48,000, respectively. The authors observed an increase in h_{TP} as the pipe was inclined from 0º to 5º, and a slight decrease in h_{TP} as the pipe was further inclined from 5º to 7º. Based on the experimental data collected and the observed h_{TP} trend, they proposed a robust correlation given below as:

$$\frac{h_{TP}}{h_L} = F_P\left\{1 + 0.55\left[\left(\frac{x}{1-x}\right)^{0.1}\left(\frac{1-F_P}{F_P}\right)^{0.4}\left(\frac{Pr_G}{Pr_L}\right)^{0.25}\left(\frac{\mu_L}{\mu_w}\right)^{0.25} I^{0.25}\right]\right\} \qquad (2.13)$$

Where h_L is from Sieder and Tate (1936), F_P is given in equation (2.12a) and I is given as:

$$I = 1 + \frac{[(\rho_L - \rho_G)gD^2|\sin\theta|]}{\sigma} \qquad (2.13a)$$

This correlation successfully predicted 72% and 85% of the experimental data within ±20% and ±30%, respectively using Chisholm (1973) void fraction correlation given in equation (2.5c).

From the detailed literature review presented, it is clear that very little work has been done to address the effect of downward pipe orientation on h_{TP}. The only work found in the literature that addresses the effect of downward pipe orientation on h_{TP} is that of Hossainy et al. (2014). Their work only covered pipe orientations ranging from 0° to -20°. Also, for the proposed correlations found in the literature, none of them specifically accounts for the effect of downward pipe orientation on h_{TP}. Although Kim and Ghajar (2006) and Tang and Ghajar (2007) were the only authors to account for the effect of pipe inclination on h_{TP} in their correlations by introducing inclination factor (I), their correlations were developed based on experimental results obtained from upward pipe orientations. Hence, this work is extremely important as it provides valuable experimental heat transfer data and analysis for the full range of downward pipe orientations (0° $\leq \theta \leq$ -90°). Also, the observed trend will enable the development of heat transfer correlation that will be able to predict h_{TP} for any downward pipe orientation independent of pipe diameter, flow patterns, and fluid combinations.

CHAPTER III

EXPERIMENTAL SETUP

In this chapter, the details of the experimental setup and a careful outline of the procedure required for collecting very good heat transfer data will be discussed. The experimental setup was designed and constructed by Cook (2008). The different parts of the setup that are going to be discussed are specific to heat transfer measurement and experiment since this is the area that the current research is focused on. This section is very important as it allows for repeatability of the experimental procedures and results. This chapter is divided into these different sections as follows: Details of experimental setup, experimental procedure, and validation of experimental setup.

3.1 Details of Experimental Setup

Figures 3.1 and 3.2 show the circuit diagram and picture of the experimental setup, respectively. The picture in Figure 3.2 is that of the experimental setup at 0^{o} inclination.

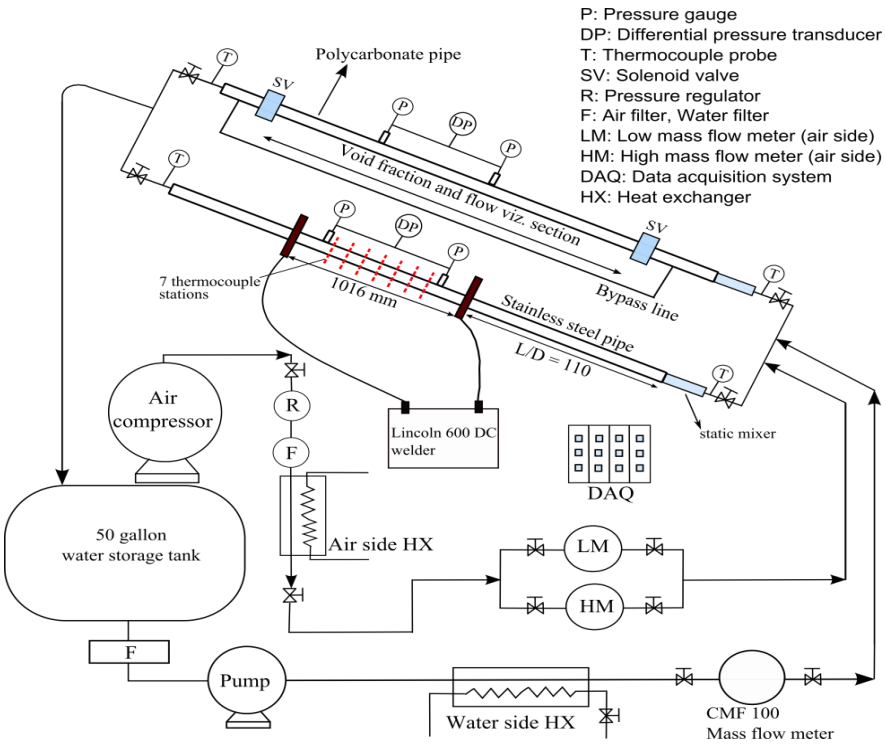

Figure 3.1 Experimental setup circuit diagram

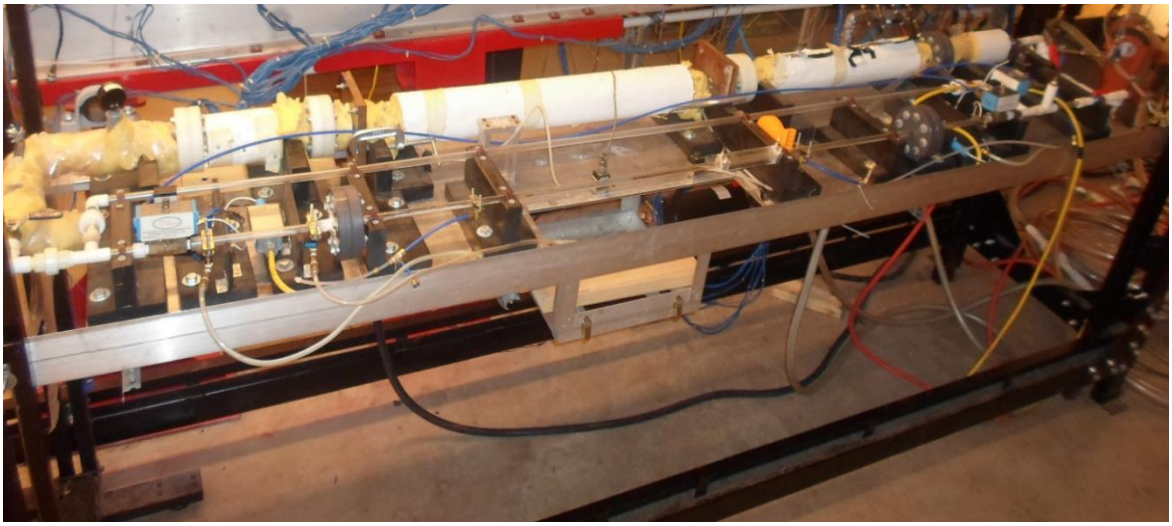

Figure 3.2 Experimental setup in 0º inclination

Test Platform: The heated branch is supported by the test platform. The platform is made of aluminium I-beam fabricated from 2.381 mm (3/32 in) aluminium and 3.175 mm (1/8 in) by 50.88 mm (2 in) aluminium angle. The dimension of the platform are 3.353 m (11ft) in length and 0.61 m (2 ft) in width. The dimension of the flat portion fabricated from the aluminium sheet are 3.05 m (10 ft) by 0.61 m (2 ft). Small holes have been cut along the lengths of the test platform to allow for various components to pass to the bottom of the platform. The heated test section is fastened to the platforms using a combination of 5.08 cm (2 in) by 15.24 cm (6 in) blocks and leather strapping. The test platform is attached to the variable inclination.

Variable Inclination Frame: The variable inclination frame allows for the heated test section to move from a maximum +90º to a minimum of -90º inclination angle. This is a very vital part of the setup as it allows research to be carried out at both near horizontal and vertical positions. This variable inclination frame consist of two frames-a heavy outer frame and a lighter internal rolling frame. The heavy frame has dimensions of 4.57m (15 ft) in length, 3.66 m (12 ft) in height and 0.84 m (33 in) in width. An extra length is allowed between the inclination frame and the test platform to accommodate any future additions to the experimental setup. The outer frame is made of 3.175 mm (1/8 in) by 50.8 mm (2 in) by 101.66 mm (4 in) of regular steel tubing. This outer frame is bolted to the floor to provide rigidity and stability of the experimental setup. The inner rolling frame is made out of 3.175 mm (1/8 in) by 38.1 mm (1.5 in) steel angle. The test platform is fastened to the rolling frame with a bolt and plastic bushing combination. Guide made out of 3.175 mm (1/8 in) by 38.1 mm (1.5 In) steel angle is attached to the upper and lower lengthwise crossbeams and also to the vertical supports at one end of the frame. This mechanism allows for positive and negative inclinations as the rolling frame is moved toward the fixed vertical supports. A protractor is used to ensure the desired angle of inclination is achieved.

Water Transport: The water used in this research is filtered through reverse osmosis. The purified water is then stored in a 208.2 L (55 gal)**.** A Bell and Gosset Series 1535 Coupled

Centrifugal Pump is used to pump water into the heated test section. Water pumped passes through an Aqua-pure AP2T water purification system. This purification system prevents growth of organic impurities and also traps foreign objects. A bypass line with a small Oberdorfer Model 600 F13 Pump and Bio Logic Bio-1.5 UV filter is also included for additional filtering to ensure that the water supplied to the heated section is completely free of organic and foreign impurities. Next, the water passes through a heat exchanger. The heat exchanger is used to maintain a constant inlet temperature of water flowing to the heated test section. The heat exchanger is constantly cooled by water supplied by a tap located in the laboratory area. After the purified water passes through the heat exchanger, it then passes through two Coriolis flow meters which control the water flow rate that goes into the heated test section. Afterwards, the water mixes with the air supply as it flows into the heated test section. The water is returned back to the 208.2 L (55 gal) reservoir via a return pipe.

Air Transport System: Air is supplied to the heated test section via an air compressor housed in a building adjacent to the lab. The compressor used is an Ingersoll-Rand T30 Model 2545 industrial air compressor. The compressor can operate at a maximum pressure and mass flow rate of 826 kPa (125 psi) and 0.25 kg/min (0.551 lbm/min), respectively. The compressor is fitted with a dump valve and an unloader valve to help maintain a consistent air pressure. Air passes from the compressor building into a 1379 kPa (200 psi) regulator/filter-drier assembly. The regulator/filter-drier assembly removes unwanted objects from the incoming air stream, prevents condensation produced by the compressor, allows for a control of the air pressure supplied to the setup, and provides additional air pressure consistency. After the air passes through the regulator/filter drier assembly, it then passes through a copper coil heat exchanger submerged in tap water. Here, the heat produced by the compressor and ambient temperature is removed. The temperature of air exiting the heat exchanger is close to the temperature of the tap water used in cooling the heat exchanger. After passing the air through the heat exchanger, the compressed air

passes through another filter-drier assembly and then through a parker Model 24NS 82(A)-V8LN-SS Needle Flow Control Valve. This meter is controlled by a system of ¼ turn ball valves. Afterwards, the air mixes with the water supply as it flows into the heated test section. The air is returned back to the 208.2 L (55 gal) reservoir via a return pipe where it is expelled from the system.

Coriolis Flow Meters: Two of the Coriolis flow meters used are the Micro Motion Elite series with accuracy of ±0.05% for liquid flow rate and ±0.2% for gas flow rate. The larger of the meter (Model CMF 100) is used to measure liquid mass flow rate in the range of 1360 kg/hr (2998 lbm/hr) to 27,200 kg/hr (59,966 lbm/hr). This meter uses a Micro Motion RFT9739 Field-Mount Transmitter to deliver reading of mass flow and other relevant fluid properties. It also transmits mass flow data to the data acquisition system via milliamp outputs. The second meter (Model CMF025) is used to monitor air mass flow rates. It can measure liquid or air mass flow rate in the range of 54 kg/hr (110 lbm/hr) to 2180 kg/hr (4806 lbm/hr). This meter uses a Micro Motion Model 1700 transmitter. It also transmits mass flow data to the data acquisition system via milliamp outputs.

Data Acquisition System (DAQ system): This is a very vital part of the experimental setup since this is where data collected from the heated section is recorded and stored on a Control Processing Unit. The National Data Acquisition system used consist of three distinct components: chassis, modules, and terminal blocks.

The chassis houses all the other components. The type of chassis used is a SCXI 1000. The main purpose of the chassis is to provide a low noise area containing components for signal conditioning, power supply, and circuitry control. This chassis is AC powered and has four slots for modules and terminal blocks.

The modules which are connected directly to the chassis carries out signal conditioning process and provide point of attachment for the terminal blocks. Two 32 channel analog modules (SCXI 1102s) and one 8 channel analog module (SCXI 1125) are used for this experimental setup. The 32 channel analog modules provides high accuracy signal conditioning of thermocouples. They can also be used to acquire data through millivolt of 0 to 20 mA, and 4 to 20 mA current signals. Each of the input channels has a 2 Hz low-pass filter for the purpose of reducing noise generated from the 60 Hz power source. Each channel also contains an amplifier with a gain in the range of 1 to 100. The 8 channel analog module is also used to acquire data from the thermocouples. This module allows for isolated analog signal conditioning via its 8 channel. Each channel contains a low-pass filter that can be configured for either 4 Hz or 10 Hz. Also, each of the 8 channels has 12 programmable gain settings ranging from 1 to 1200.

The terminal block provides a direct connection for the thermocouples and Coriolis flow meters. Twin shielded SCXI 1303 32 Channel Isothermal Terminal Blocks are used to connect the SCXI 1102 modules. These terminal blocks are front mounted and provide direct connection to the modules through screw terminals. For high accuracy of measured data, they have an isothermal construction, and contain an on-board temperature sensor for cold junction compensation. For the 8 channel module, a SCXI 1313 High Voltage Attenuator Terminal Block is used. Similar to the 32 channel terminal blocks, it has an additional 100:1 resistive voltage divider which allows for the terminal blocks to accept inputs of up to ±300 VDC when the terminal block is used with the SCXI 1125 module.

A CPU is used to record and store data. A graphical interface program, LABVIEW, designed by National Instrument is used for data acquisition. This program was originally written by Jae-young Kim and later modified by Clement Tang.

Connection to the Test Area: Air and water are carried to the test section area via reinforced flexible tubing. To transport air and water to the inlet of the test area, a standard 3/8 in nominal air compressor hose and a 1 1/8 in nylon reinforced flexible clear PVC tubing are used respectively. The water and air enters the test area via a 1/2 in IPS plastic tee where they begin to mix. Further mixing of air and water is accomplished by use of a static mixer. One arm of the plastic tee goes to the heated test section area. Flow into this area is controlled by 1/2 in quarter turn ball valves. The two phase flow mixture passes through the heated test section area and exist via a 1/2 in CPVC. Two ball valves are placed at the exit of the test section area to prevent back flow into unused test branch as shown in Figure 3.1.

Mixing Section: A koflo 3-Vane static mixer (Model 3/8-40C-4-3V-2) made from 3/8 in nominal clear PVC is used at the inlet of the test section. This mixer ensures that the air and water that flows into the heated section is mixed properly so that an accurate temperature of the mixture can be read by the thermocouple probe. The mixer also ensures that the two phase flow patterns observed are not influenced by entry configuration. After the air and water passes through the inlet mixer, it flows through the heated test section and exit through an outlet mixer. The outlet mixer is a Koflo 1/2-80-4C-3-2. Similar to the inlet mixer, the outlet mixer ensures that a proper outlet temperature of the air-water flow is measured by the thermocouple.

Flow Visualization Section: This section is made out of a 1.27 cm (0.50 in) ID polycarbonate tubing. The wall thickness of the tubing is 1.59 mm (1/16 in). The polycarbonate material used provides optical clarity and thermal resistance. Optical clarity is important to ensure that clear photos of the flow patterns are taken. Also, it is necessary that the material can provide high thermal resistance since the flow visualization sections are in direct contact with the heated test section. The polycarbonate flow visualization sections provide temperature resistance of up to 132 ºC (270 ºF). Flanges which were made out of a 2.54 cm (1 in) thick PVC material are used to connect the polycarbonate flow visualization section with the PVC test section. Also, flanges that

needed temperature resistance were made out of a 2.54 cm (I in) thick nylon stock which provided these flanges a temperature resistance of up to 110 ºC (230 ºF). Each of these flanges has a diameter of 15.24 cm (6 in). An O-ring system is used to seal off the flanges. One of the O-rings sits behind the polycarbonate lip and the other sits on the face of the flanges. On the other side of the flange, a threaded joint is used to attach the flange to the PVC pipe. A PVC female threaded union is glued into the side if the flange system to be joined with the PVC pipe. This enables the attachment of a PVC male nipple to the flange.

Heated Section: This section is made of 3/8 in nominal schedule 40 IPS alloy 304 stainless steel pipe. It has an actual diameter of 12.52 (0.493 in) and length of 80 diameters or 101.6 cm (40 in). The section is heated by passing high amperage current which ensures that a uniform wall heat flux is generated. Current is supplied via a Miller Maxtron 450 arc welder which produces up to 450 A at 100 % duty cycle. A 6.35 mm (1/4 in) thick copper plates which were silver soldered at either end of the test section is used to provide electrical connection. The plates completely encircle the test section and are 17.8 cm by 17.8 cm (7 in by 7 in) in order to achieve an even distribution of current input to the heated test section. In order to prevent heat loss from the heated test section, a 1.27 cm (0.5 in) thick phenolic resin board is used on the sides of the plates that faces away from the heated section. A 4/0 AWG welding cable is used to connect the plates and the welder. Also, a 1000 amp shunt (Manufactured by Empro Shunts, Model number B-1000-50) is connected in line with the circuit at the exit side of the connection plate.

Thermocouple Array: Thermocouple probes and glued-on thermocouples are used to measure temperature at the inlet, exit, and along the length of the heat test section. The thermocouples used for this experimental setup are of type T and they each produce an accuracy of the greater of either ±1.0 ºC (1.8 ºF) or ±0.75% of the measured value. These thermocouples have a working temperature range between -250 ºC (-418 ºF) and 350 ºC (662 ºF). The thermocouples and thermocouple probes are wired to the data acquisition system using a 6.1 m (20 ft) length of

Omega 24 gauge type T thermocouple wire (EXTT-T-24-SLE). Omega TMQSS-062U-6 thermocouple probes are used at the inlet and exit of the heated test section branch. These probes are inserted into the test branch extending downwards to the bottom of the inner wall of the branch. This is done to ensure that an accurate temperature of the two phase flow mixture is measured. The probes are sealed into the test branch using compression fittings.

The glued-on thermocouples used are Omega CO1-T thermocouples. These thermocouples are laminated between two thin layers of phenolic resin so as to provide shielding from electrical disturbance. These thermocouples were attached to the test section using Omega bond 101 two-part thermocouple epoxy. This type of epoxy provides high thermal conductivity of 1.038 W/m.K (7.2 BTU-in/hr-ft²-ºF). Thermocouples were attached in sets of four, consisting a North, South, Ease, and West placement scheme at each point of measurement. Starting at 12.7 cm (5 in) from the first copper connection, seven sets of thermocouple were placed at intervals of 12.7 cm (5 in) across the entire length of the test section in a symmetrical configuration. This type of thermocouple array allows for temperature measurements around the circumference of the heated section as well as along its length. In order to prevent heat loss, the test section is covered with a 7.62 cm (3 in) thick Micro-lok Fiber Glass Pipe Insulation. The insulation used has a conductivity of 0.042 W/m.K (0.29 Btu in/ (hr-ft²-ºF) at 93 ºC (200 ºF). The rest of the heated test section is wrapped in three layers of Thermwell Fiber Glass Pipe Insulation Wrap. Each layer of this insulation has an R-value of 1.6.

Data Reduction: For a uniform wall heat flux boundary condition, the experimental setup used for this work measures the outside wall temperatures at four circumferential intervals separated by $\pi/2$ radian, inlet and outlet bulk temperatures, voltage, and current. The inside wall temperature is not measured directly, but is calculated from the outside wall temperature and heat generation using the data reduction program which has been developed by Ghajar and Kim (2006). This is achieved by applying a finite difference method on a control volume. After

calculating the inside wall temperature, the local heat transfer coefficient is determined from the local inside wall temperature, local bulk fluid temperature, and local inside wall heat flux. The overall heat transfer coefficient is evaluated by integrating the local average heat transfer coefficient along the pipe length as shown in Equation (3.1). The Nusselt number is calculated from the overall heat transfer coefficient obtained in Equation (3.1) as shown in Equation (3.2).

$$h = \frac{1}{l}\int \bar{h}\,dz = \frac{1}{l}\sum_{j=1}^{N_{ST}} \bar{h}_j \Delta z_j \tag{3.1}$$

$$Nu = \frac{hD_i}{k} \tag{3.2}$$

In this experiment, to ensure accuracy and reliability of the experimental data, it is imperative that a low heat balance error is maintained (preferably below ±10% for two phase heat transfer coefficient). The heat balance error is the percentage difference between the heat input rate from the welder and heat transfer rate calculated by using the enthalpy equation for the flow. These are given as:

$$\text{Heat input rate, } \dot{q} = V_D I \tag{3.3}$$

$$\text{Heat rate from enthalpy, } \dot{q} = \dot{m}c(T_{b,out} - T_{b,in}) \tag{3.4}$$

$$\text{Heat balance error (\%)} = \frac{Heat\ rate\ from\ enthalpy - Heat\ input\ rate}{Heat\ input\ rate} \times 100 \tag{3.5}$$

3.2 Experimental Procedure

Start-up Procedure:

1) Ensure that the valves in the heated test section are open to allow for inflow and outflow of air and water.
2) Check the air and water filter to ensure they are working properly and that they are not clogged up with dirt. Next, turn on the tap water to allow for the stabilization of temperature of the incoming air and water that will be used for the experiment.

3) Turn on the water Coriolis flow meter, air compressor, air regulator, and DAQ system. It is important to make sure that there is a continuous inflow and outflow of the air-water mixture in the heated test section. Also check the setup to make sure that there are no leaks.
4) Check all the electrical wires and connections of the DC welder, the copper plates, and the DAQ system and ensure that they are in good condition. Replace or change any burnt or bad wire. After successfully executing the above steps, the setup is ready to be used for collecting experimental data as outlined below.

Measurement Procedure:

1) Set the water and air flow rate to the desired value via the Coriolis meter. Next, ensure that the "Welder power status" button on the LabVIEW software graphical interface is turned on as shown in Figure 3.3. Then, click the run button on the LabVIEW software interface so as to save the data file.
2) Check the water and air Reynolds numbers, water and air flow rates, temperature of the thermocouple stations, the inlet and outlet thermocouple probes temperatures, and the system pressure displayed by the LabVIEW software graphical interface as shown in Figure 3.3 and ensure they correspond with the expected values.
3) Before turning on the DC welder, allow some time for the inlet and outlet temperature of the air-water mixture to stabilize. A temperate difference of less than 0.3 ºC is preferred so as to minimise the heat balance error.
4) Next, turn on the DC welder and set it to a value which will ensure a minimum temperature difference between the inlet and outlet temperature of 4 ºC. This is important to allow for collection of a healthy heat transfer data. Allow for the system to achieve steady state. Steady state is assumed to be achieved if the variation of the temperature of both the inlet and outlet thermocouple probe is less than 0.5 ºC within 5 minutes.

5) Next, press the record button on the LabVIEW software as shown in Figure 3.3. The time given to recording a data point can vary from 3 minutes to 10 minutes depending on the flow pattern.
6) After recording the data, press the stop button and turn off the record button on the LabVIEW software graphical interface.
7) Turn off the DC welder and allow the system to cool down. Repeat steps 1 through 6 for the remaining data points.

Shut Down Procedure:

1) After collecting experimental data, turn off the DC welder, the air and water Coriolis flow meter, the tap water, pressure regulator and the DAQ system.
2) Turn off the air compressor located outside the laboratory building.
3) Ensure that the DC welder and Coriolis flow meters are set to their minimum values before exiting the laboratory.

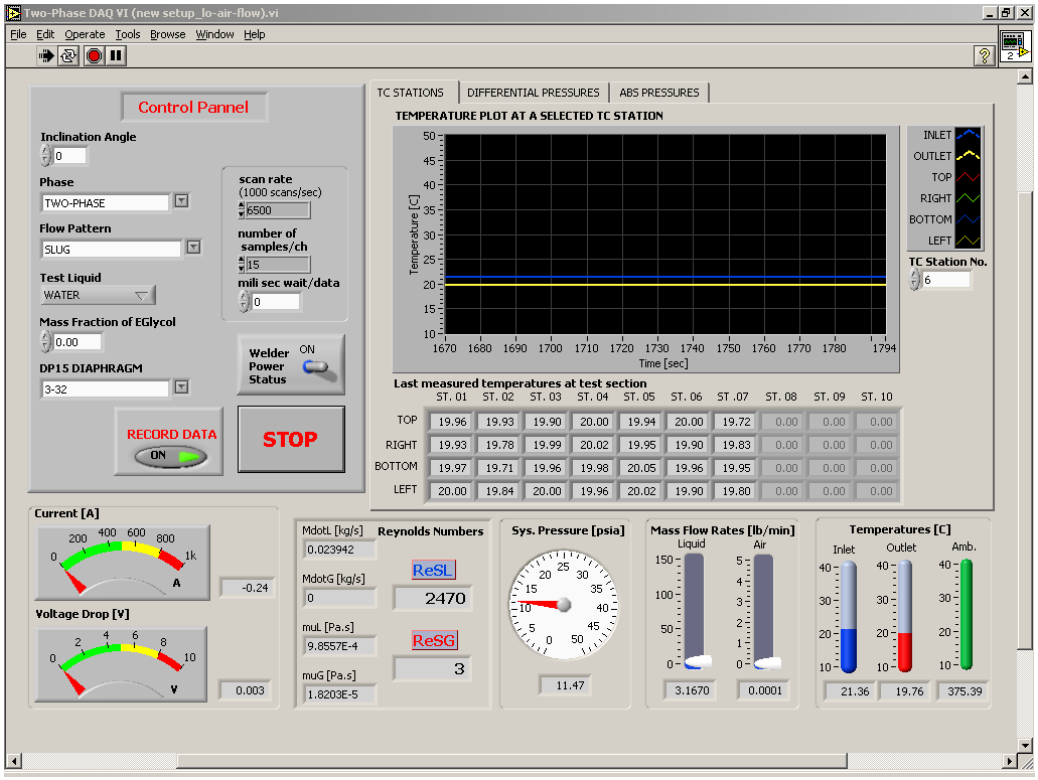

Figure 3.3 LabVIEW software graphical interface

3.3 Validation of the Experimental Setup

3.3.1 Two Phase Heat Transfer Uncertainty

The uncertainty in measurement of two phase heat transfer coefficient and other associated two phase flow variables is shown in Table 3.1 for a sample run. The minimum and maximum uncertainty associated with each flow pattern is also shown in Table 3.2. These uncertainties are calculated using the method proposed by Kline and McClintock (1953). Details of the uncertainty calculations are presented in Appendix A. The higher magnitudes of uncertainty in stratified (31.52%), intermittent (28.34%) and annular (25.35%) flows are due to inability to maintain a higher temperature difference across the pipe inlet and exit and the higher values of heat balance error associated with these flow patterns.

Table 3.1 Uncertainty in measured values of two phase heat transfer coefficient

Variable	Value	(±) Uncertainty (%)	(±) Uncertainty (%)
Inner Diameter (m)	0.0125	1.27E-5	0.10
Outer Diameter (m)	0.0171	1.27E-5	0.07
Length (m)	1.016	3.175E-3	0.31
Thermal Conductivity (W/mK)	13.438	–	–
Current (A)	245	2.45	1.00
Voltage (V)	1.9	0.019	1.00
Thermal Resistance (K/W)	0.0036	1.85E-5	0.51
Inner Wall Temperature (°C)	13.87	0.55	3.96
Heat Flux (W/m^2)	11672	195	1.67
Heat Transfer Coefficient (W/m^2K)	3065	967	31.54

Table 3.2 Minimum and maximum uncertainty in measured h_{TP} for different flow patterns

Flow pattern	Minimum uncertainty (%)	Maximum uncertainty (%)	Average uncertainty (%)
Stratified	0.96	31.52	10.27
Slug	2.23	13.39	7.82
Intermittent	0.57	28.34	9.74
Falling Film	1.87	4.78	3.32
Bubbly	2.42	11.59	9.25
Annular	1.09	25.35	3.98

3.3.2 Comparison of Single Phase Heat Transfer Measurements with Correlations

In this section, the validity of the experimental setup will be determined by comparing the single phase heat transfer data acquired from the setup against three correlations: Dittus and Boelter (1930), Ghajar and Tam (1994), and Seider and Tate (1936). These correlations are listed in Table 3.3. 11 data points in the Re_L range of 6800 to 25000 is compared against these correlations. From Figure 3.4, it can be seen that the experimental data points are within ±10% of Seider and Tate (1936). Also, the absolute maximum and mean error of the single phase heat transfer experimental data with respect of Dittus and Boelter (1930), Ghajar and Tam (1994) and Seider and Tate (1936) are given as 13.67%, 9.58%; 12.28%, 7.9%, and 6.09%, 2.35% respectively. All the single phase experimental data fall within ±15% of all three correlations which is within the

acceptable range of error. Hence, the experimental setup is working properly and can be used to collect two phase heat transfer data.

Table 3.3 List of single phase heat transfer correlations

Source	Single phase heat transfer correlations
Dittus and Boelter (1930)	$Nu_L = 0.023Re^{\frac{4}{5}}Pr^n$ Where n = 0.4 for heating
Ghajar and Tam (1994)	$Nu_L = 0.023Re^{0.8}Pr^{0.385}(l/D_i)^{-0.0054}(\mu_b/\mu_W)^{0.14}$
Seider and Tate (1936)	$Nu_L = 1.86(Re_{SL}Pr_L\ \frac{D_i}{l})^{\frac{1}{3}}$ (L) $Nu_L = 0.023Re_{SL}{}^{0.8}Pr_L{}^{0.4}(\frac{\mu_b}{\mu_W})^{0.14}$ (T)

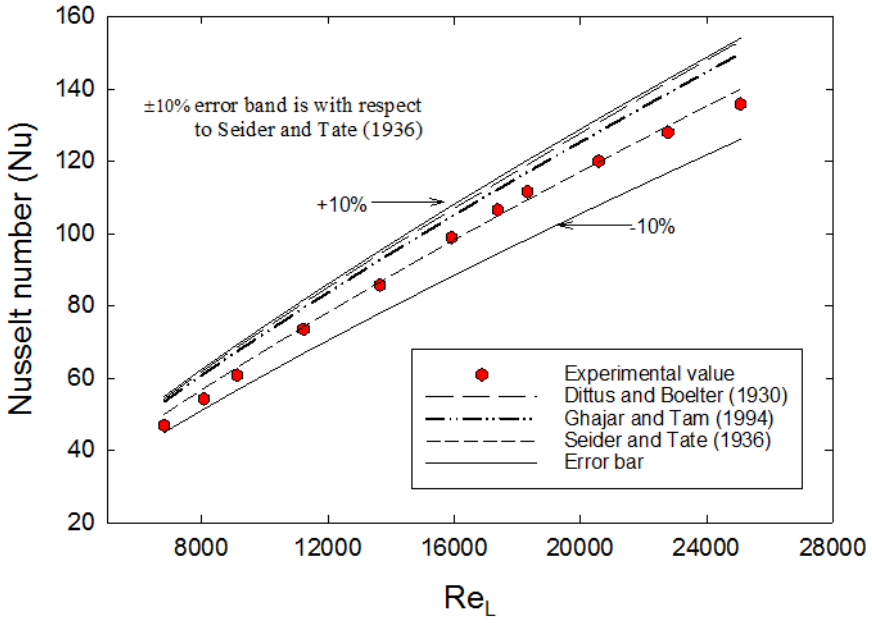

Figure 3.4 Comparison between measured and predicted values of single phase heat transfer coefficient

3.3.3 Comparison of Two phase Heat Transfer Measurements with Past Work

In this section, a sample of some two phase data points for 0°, -5°, -10º and -20° collected and compared against past work are presented. Measurement were carried for low (Re_{SL} = 2500) and moderate (Re_{SL} = 8000) superficial liquid Reynolds number and compared with the work of Hossainy et al. (2014). As shown in Figure 3.5, there was a close match of heat transfer trend of the present work and the work of Hossainy et al. (2014) for 0°, -5°, -10º and -20°. The maximum, minimum, and absolute average h_{TP} percentage difference between the present work and that of Hossainy et al. (2014) are tabulated in Table 3.4. High percentage difference is observed for low Re_{SL} and high Re_{SG} due to high disturbance observed in this flow region and the presence of high volume of gas which increases the heat balance error and thus the percentage uncertainty. Overall, the absolute average h_{TP} percentage difference is found to be less than 11%. Hence, the experimental procedure for two phase flow is highly repeatable and the setup is working properly.

Table 3.4 Comparison of h_{TP} % difference of present work and that of Hossainy et al. (2014)

Inclinations	(±) Minimum h_{TP} % difference		(±) Maximum h_{TP} % difference		(±) Absolute Average h_{TP} % difference	
	Re_{SL} = 2500	Re_{SL} = 8000	Re_{SL} = 2500	Re_{SL} = 8000	Re_{SL} = 2500	Re_{SL} = 8000
0°	0.07	1.56	20.14	10.34	6.68	7.30
-5°	2.64	0.17	16.74	11.53	10.45	6.77
-10°	1.36	0.07	9.27	7.54	4.41	4.22
-20°	0.43	0.13	19.15	9.54	7.17	5.73

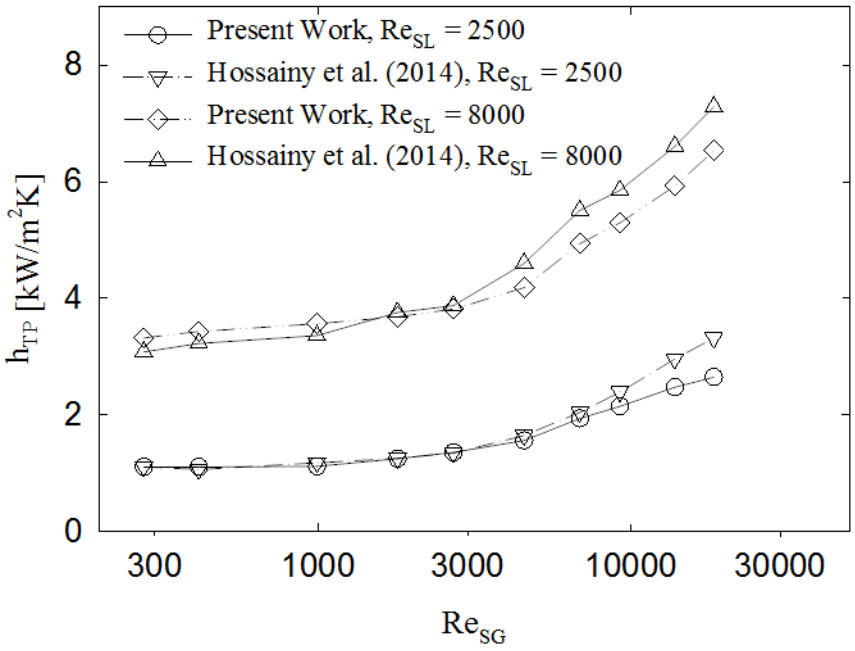

(a) 0°

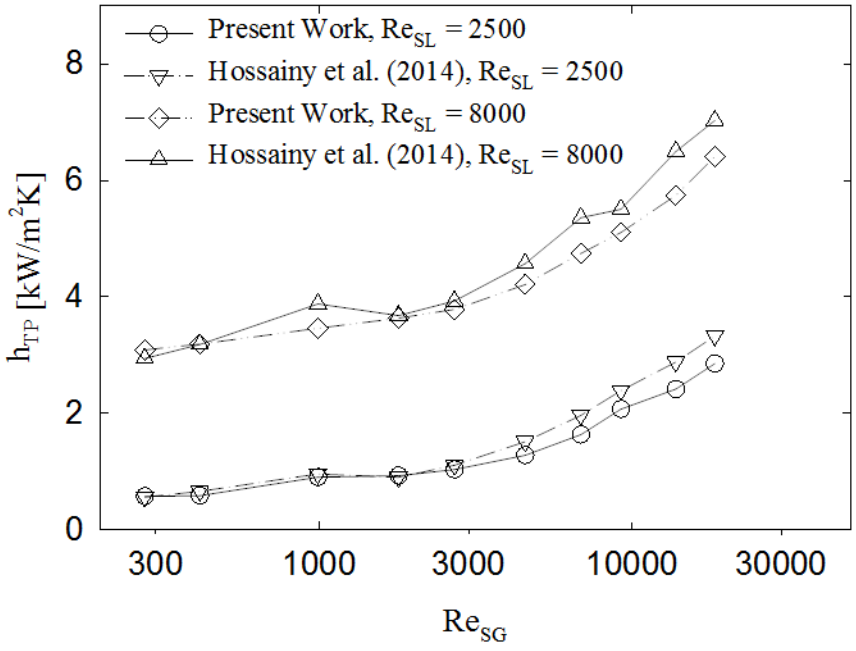

(b) -5°

Figure 3.5 (Continued on the next page)

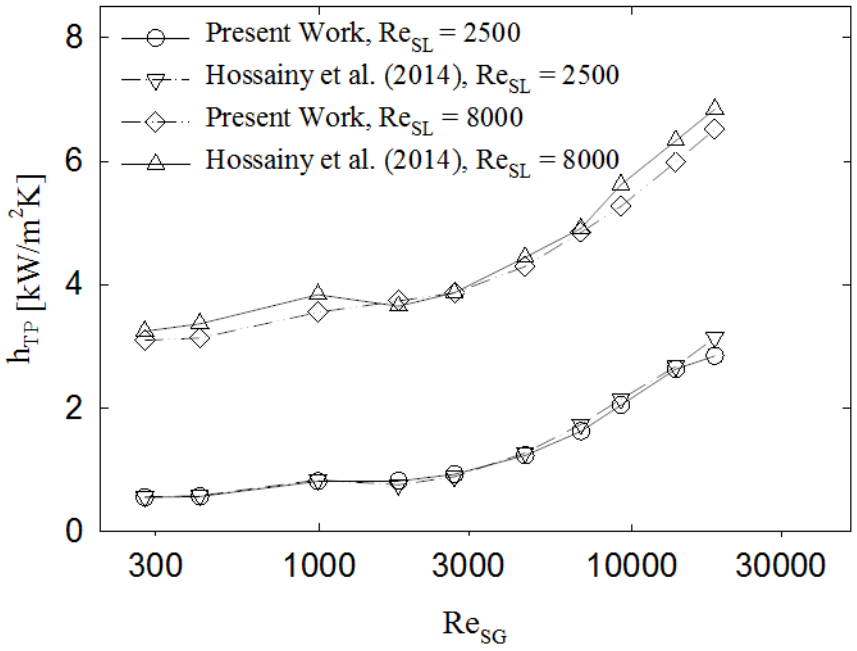

(c) -10°

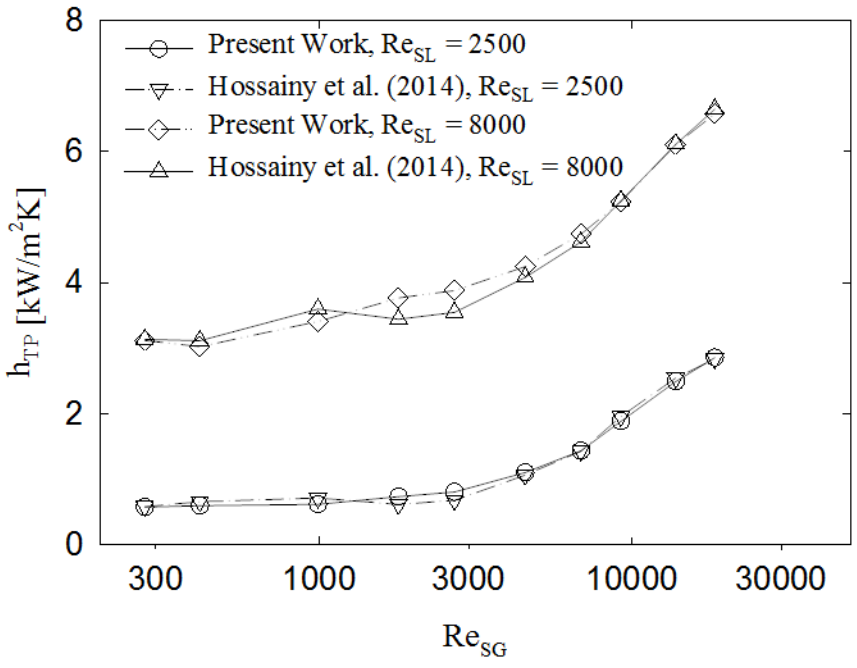

(d) -20°

Figure 3.5 Comparison of selected data points with that of Hossainy et al. (2014)

CHAPTER IV

RESULTS AND DISCUSSION

In this chapter, a detailed analysis of the experimental results will be presented. The first section titled “Flow Patterns” will present and discuss the structure of the various flow patterns observed in this study. The second section titled “Heat Transfer” is divided into four subsections. The first subsection titled “Effect of Flow Patterns and Phase Flow Rates on h_{TP} (two phase heat transfer coefficient)” will address how the flow patterns and phase flow rates affect and influence the heat transfer coefficient for downward pipe inclinations ($0^o \leq \theta \leq -90^o$). Next, the second subsection titled “Effect of Flow Patterns and Pipe Inclination on h_{TP}” will discuss how h_{TP} varies as the pipe is inclined from 0^o to -90^o and the role different flow patterns play in the observed h_{TP} trend. The third subsection titled “Analysis of Heat Transfer Correlations Performance” will discuss the performance of selected heat transfer correlations shown in Table 4.1 against experimental data obtained from this work. The best performing correlations will be identified. Finally, the last subsection titled “Correlation Development” will discuss the proposal of an improved correlation to better predict h_{TP} trend for downward pipe inclination based on the results obtained in the previous subsection.

4.1 Flow Patterns

Gas-liquid two phase flow patterns that are generated due to phase density difference, compressibility nature of the gas phase and the interaction between body and surface forces influence the parameters of practical interest such as void fraction, pressure drop and heat transfer. Thus, it is very important to have an idea of the physical structure of key flow patterns observed in horizontal and downward pipe inclinations. In the present study, two phase flow patterns are observed in a 12.7 mm I.D. polycarbonate transparent pipe that runs parallel to the heat transfer test section. The flow patterns are observed at similar flow rates to that of heat transfer measurements. Overall for all pipe orientations considered in this study ($0^o \leq \theta \leq -90^o$), six major flow patterns namely bubbly, slug, intermittent, falling film, stratified and annular flow are observed. Representative pictures of these flow patterns are shown in Figure 4.1.

The bubbly flow that occurs at moderate to high liquid flow rates and low gas flow rates is characterized by numerous bubbles (gas phase) dispersed in a continuous liquid phase. These bubbles can vary in size, shape and distribution depending on the pipe orientation and phase flow rates. The gas phase in form of bubbles is concentrated in the vicinity of the pipe upper wall due to the buoyancy acting on the gas phase whereas they appear to be evenly distributed around the pipe axis for vertical downward flow. The slug flow is characterized by long cylindrical pockets of gas trapped in a continuous liquid phase that flow in an intermittent manner with a certain frequency. The frequency and length of the gas slug depends on the phase flow rates, fluid properties and pipe inclination. For horizontal and near horizontal downward inclinations, the gas slug is in the vicinity of the pipe upper wall whereas, for near vertical downward flow, the gas slug appears axisymmetric. Depending upon the relative magnitude of buoyancy and inertial forces, the gas slug nose may have a bullet shaped, blunt or flat nose. The intermittent flow in this study is defined as the flow pattern characterized by the turbulent and chaotic behavior of two phase flow with significant mixing between the two phases. Using this description, the flow

pattern in the vicinity of the transition lines such as slug-wavy, stratified-rolling wave and annular-wavy flow patterns are classified as intermittent flow patterns. The falling film flow occurs at vertical and near vertical downward pipe orientations and is a special case of stratified flow. Unlike stratified flow, the entire pipe circumference is wetted by a thin liquid film that surrounds the central gas core. Visually, the falling film flow appears similar to the annular flow pattern however; the two flow patterns are significantly different in terms of the liquid film characteristics, inertia of the central gas core and momentum exchange at the gas-liquid interface. The stratified flow that occurs at low to moderate gas and liquid flow rates is characterized by the flow of gas and liquid phase moving in two separate layers (gas phase on top of liquid phase) in the pipe. Stratified flow predominantly exists in horizontal and downward pipe inclinations. The stratified flow can be classified as smooth stratified and wavy stratified. In smooth stratified flow, the gas-liquid interface is flat while the wavy stratified flow is characterized by the generation of disturbance waves that grow on the gas-liquid interface and occasionally touch the pipe upper wall. Finally, the annular flow pattern that appears at low liquid flow rates and high gas flow rates can be described as flow of rough and wavy liquid film in the vicinity of the pipe wall that surrounds the central fast moving gas core. Annular flow is one of the most studied, widely observed and a very important flow pattern since it is known to significantly enhance the heat transfer compared to the single phase flow.

In this study, two phase heat transfer coefficients are measured for all aforementioned flow patterns in horizontal and downward pipe inclinations by varying gas and liquid mass flow rates (phase superficial Reynolds numbers) in a range of 0.001-0.2 kg/min ($270 \leq Re_{SG} \leq 19000$) and 1-10 kg/min ($2300 \leq Re_{SL} \leq 17000$), respectively. The superficial Reynolds numbers for liquid and gas flow rates are defined by Equations (4.1) and (4.2), respectively where x is the two phase flow quality and G is the total two phase mixture mass flux.

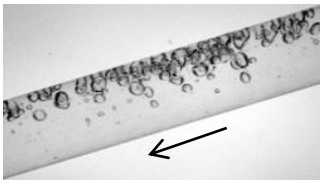

(a) Bubbly

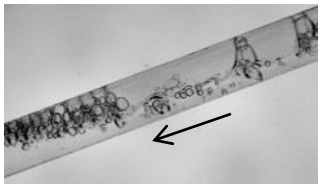

(b) Slug

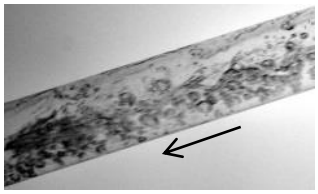

(c) Intermittent

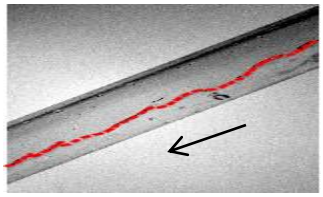

(d) Stratified

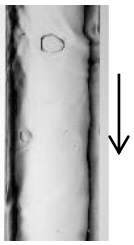

(e) Falling film

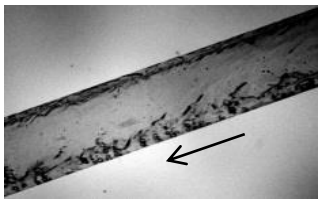

(f) Annular

Figure 4.1 Flow patterns observed in downward inclined two phase flow (John et al. (2015))

$$\mathrm{Re}_{SL} = \frac{\rho_L V_{SL} \mathrm{D_i}}{\mu_L} = \frac{G(1-x)\mathrm{D_i}}{\mu_L} \tag{4.1}$$

$$\mathrm{Re}_{SG} = \frac{\rho_G V_{SG} \mathrm{D_i}}{\mu_G} = \frac{Gx\mathrm{D_i}}{\mu_G} \tag{4.2}$$

4.2 Heat Transfer

4.2.1 Effect of Flow Patterns and Phase Flow Rates on h_{TP}

The variations of two phase heat transfer coefficient (h_{TP}) with change in superficial gas and liquid Reynolds numbers (Re_{SL} and Re_{SG}) for horizontal (θ = 0º) and downward inclined pipe orientations (θ = -5º, -10º, 20º, -30º, -45º, -60º, -75 and -90º) are shown in Figure 4.2. For all pipe inclinations (0º ≤ θ ≤ -90º), in general, it is found that the two phase heat transfer coefficient increases with increase in gas and liquid flow rates. However, it is important to note that the nature of increment of h_{TP} depends

on flow patterns as a function of gas and liquid flow rates. It is observed that independent of the pipe orientation, for low liquid flow rates ($Re_{SL} \leq 4000$), increment in h_{TP} is insensitive to the increase in gas flow rates approximately up to $Re_{SG} < 5000$. This region typically consists of slug and stratified flow patterns. In this region, the physical structure of the slug flow is influenced by the dominant buoyant force (acting on the gas phase) in the direction opposite to that of the mean flow. The dominant buoyant force decreases the slug translational velocity and hence increases its residence time in the test section. The slower moving gas slug offers resistance to the heat transfer from pipe wall to the two phase mixture. Consequently, the two phase heat transfer coefficient increases only marginally with increase in the gas flow rates. In comparison to the slug flow in horizontal and downward pipe inclinations, the heat transfer coefficient in vertical downward slug flow increases more rapidly with increase in Re_{SG}. This trend is expected to be a result of axisymmetric distribution of the two phase flow in vertical downward pipe inclination. As shown in Figure 4.3, the gas slug (with nose pointing upward, flat and downward) is surrounded circumferentially by a thin liquid film in contact with the pipe wall. This thin liquid film permits higher heat transfer rates compared to that in horizontal and downward pipe inclinations where only a fraction of pipe circumference is in contact with a relatively thick layer of liquid while the remaining portion is in contact with the gas slug. In case of stratified flow regime, there is no coupling between the two phases (i.e., the two phases flow separately in layers with gas phase on top of liquid phase) and at low gas and liquid flow rates, there is no driving force for the gas phase against dominant buoyant force. As a result, the two phase heat transfer coefficient depends virtually on the liquid flow rate. For a fixed pipe orientation, increase in liquid flow rate increases the circumferential fraction of the pipe (wetted perimeter) in contact with the liquid phase and makes the velocity profile of the liquid layer steeper and hence eventually results in the increase in two phase heat transfer coefficient. In case of intermittent and annular flow patterns, a sharp increase in h_{TP} is observed with increase in the gas and liquid flow rates.

A close observation of the trends of h_{TP} in intermittent flow pattern reveals that during the onset of intermittent flow, h_{TP} initially increases gradually with increase in Re_{SG} typically up to $Re_{SG} \approx 5000$ and then increases rapidly with increase in the superficial gas Reynolds number. This is probably due to the difference in the physical structure of the sub regions of intermittent flow pattern. At low Re_{SG}, the physical structure of intermittent flow pattern is slug wavy in nature whereas for higher Re_{SG}, the intermittent flow regime features chaotic, turbulent characteristics resembling annular wavy flow. Thus, the steeper trends of h_{TP} at higher Re_{SG} in intermittent flow regimes are possibly due to higher level of turbulence and interfacial interaction between the two phases.

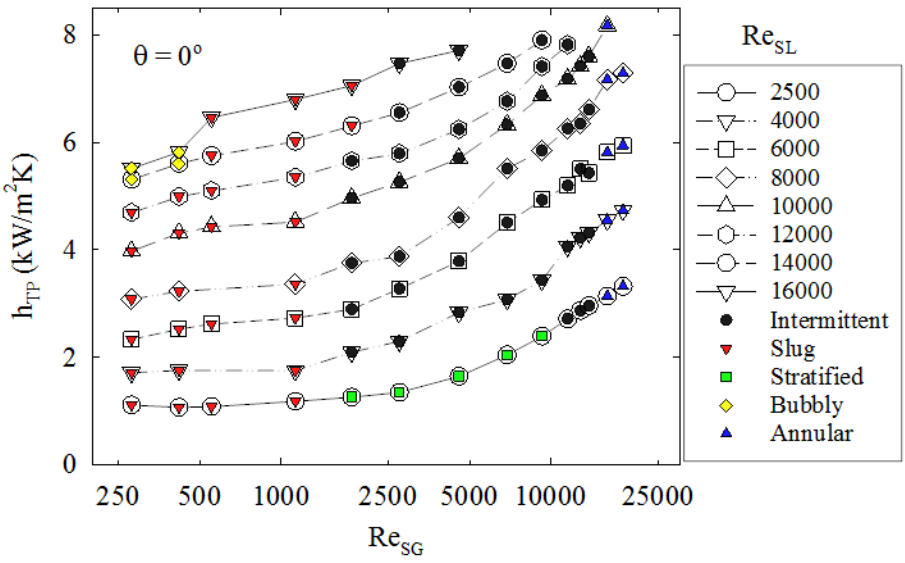

(a)

Figure 4.2 (Continued on the next page)

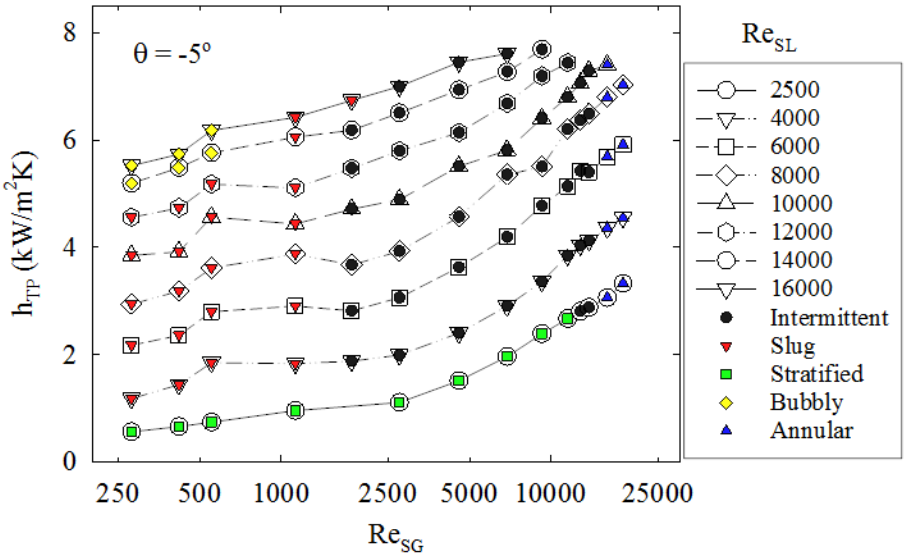

(b)

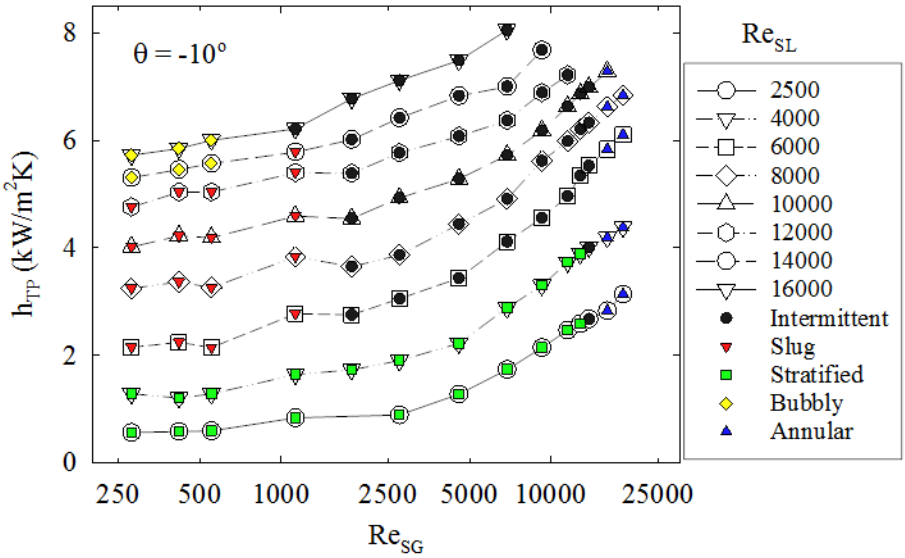

(c)

Figure 4.2 (Continued on the next page)

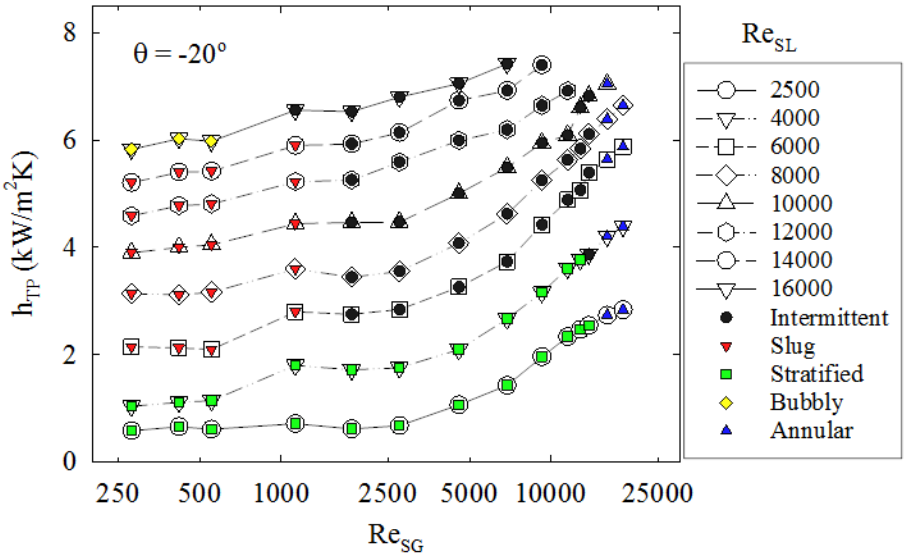

(d)

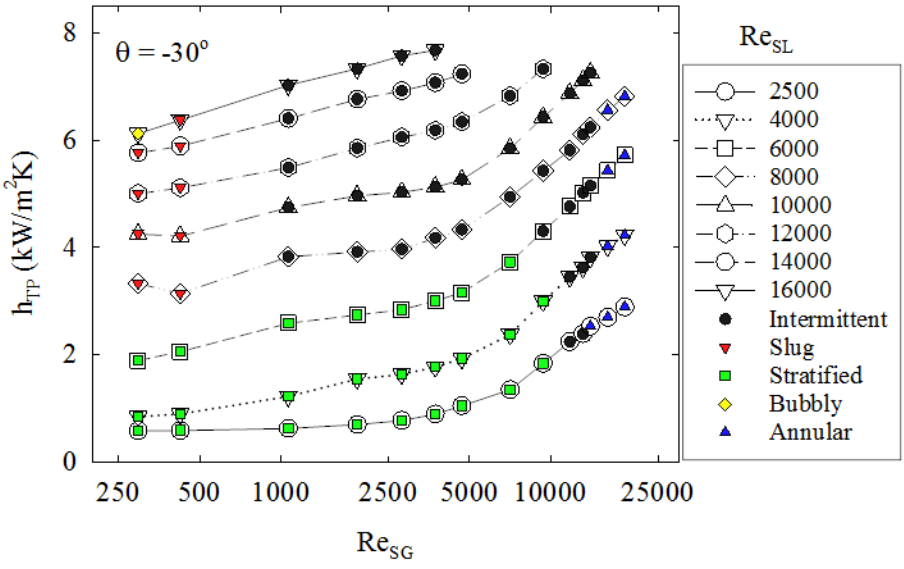

(e)

Figure 4.2 (Continued on the next page)

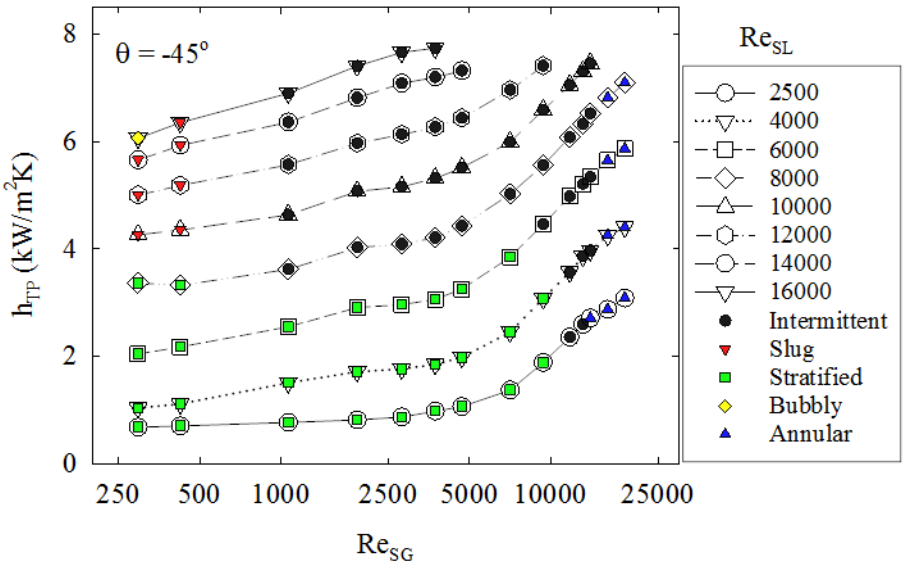

(f)

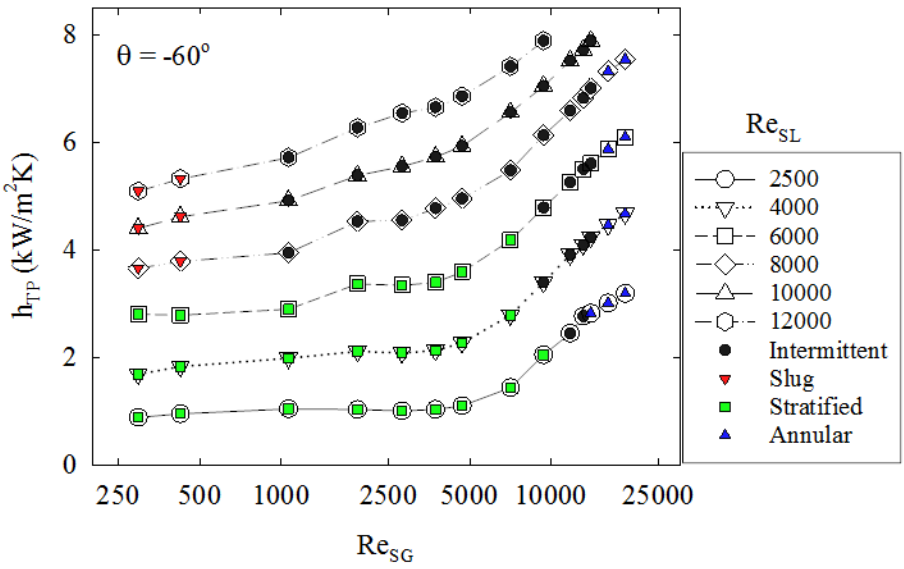

(g)

Figure 4.2 (Continued on the next page)

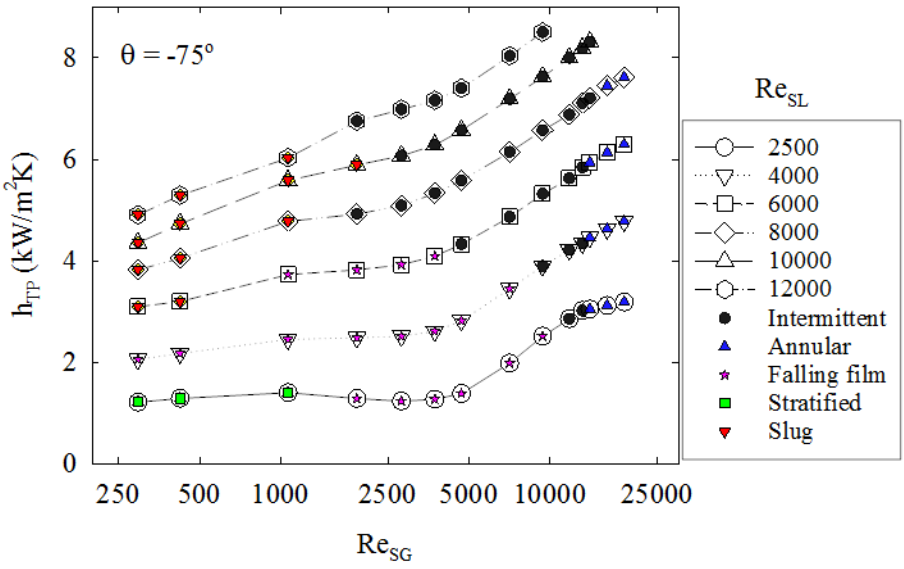

(h)

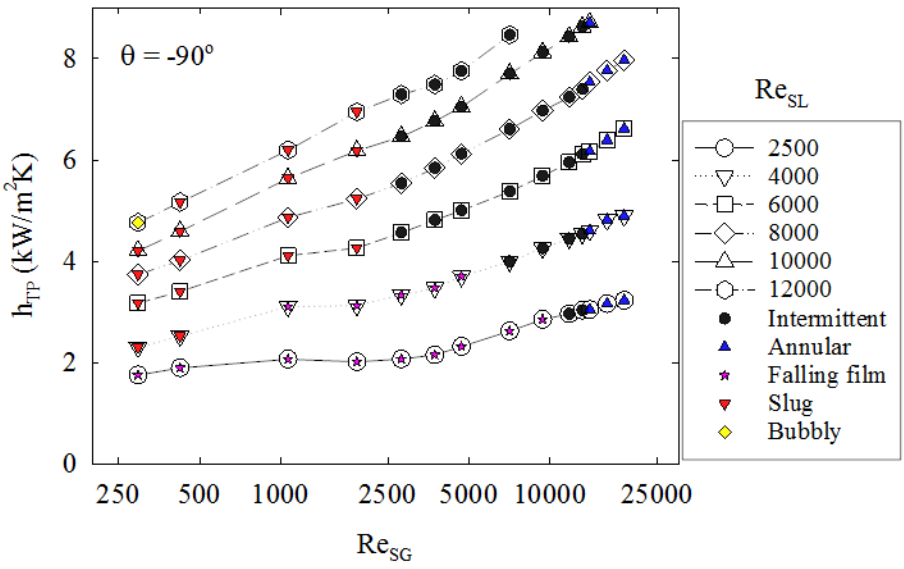

(I)

Figure 4.2 Variation of h_{TP} with change in Re_{SL} and Re_{SG} in horizontal and downward inclined two phase flow

In annular flow regime, the two factors that most likely contribute to a rapid increase in two phase heat transfer coefficient are the interfacial disturbance waves and thickness of liquid film in contact

with the pipe wall. The onset of annular flow is characterized by the sweeping action of the disturbance waves at the gas-liquid interface. The amplitude of these disturbance waves is large enough to momentarily bridge the entire pipe cross section. The increase in amplitude and frequency of disturbance waves with increase in gas and liquid flow rates increases the sweeping action and hence the level of turbulence at the gas-liquid interface. Secondly, the thickness of liquid film (in contact with the pipe wall) decreases with increase in the gas flow rate. A decrease in liquid film thickness reduces the resistance to the heat transfer from pipe wall and results into steeper velocity and temperature distributions. Both of these factors favor higher heat transfer and hence show a rapid increase in h_{TP} with increase in Re_{SL} and Re_{SG}.

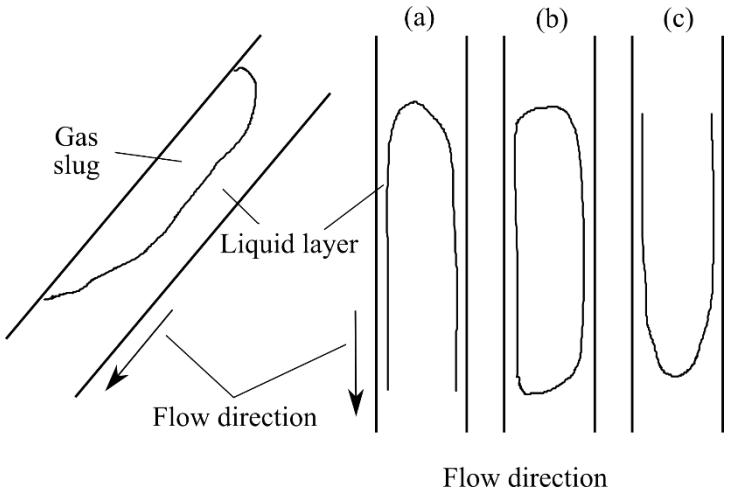

Figure 4.3 Physical structure of slug flow in downward inclined and vertical downward two phase flow (a) upward slug nose (b) flat slug nose (c) downward slug nose. (John et al. (2015))

4.2.2 Effect of Flow Patterns and Pipe Inclination on h_{TP}

An increase in downward pipe inclination (θ) from horizontal is known to significantly affect the two phase heat transfer coefficient (h_{TP}) essentially due to the balance between buoyancy, gravity and inertial forces. Figure 4.4 shows the variation of h_{TP} as a function of Re_{SL} and Re_{SG} for the horizontal and downward pipe inclinations of -5°, -10°, -20°, -30°, -45°, -60°, -75° and -90°. With reference to the horizontal flow direction, the two phase heat transfer coefficient is found to decrease with

increase in downward pipe inclination and a minimum is observed in between -30º and -45º of pipe inclinations. Although the h_{TP} at -45º is slightly greater than that at -30º, this difference appears to be well within the experimental uncertainty. For low Re_{SL} and Re_{SG} values, a maximum of 47% decrease is observed in h_{TP} at -30º with reference to that at horizontal pipe orientation. With further increase in downward pipe inclination beyond -45º, the two phase heat transfer coefficient increases consistently with maximum h_{TP} observed for vertical downward (θ = -90º) two phase flow.

The average decrease in h_{TP} for fixed Re_{SL} of 2500 and varying Re_{SG} is about 30%. It is evident from Figure 4.4 that the effect of pipe orientation on the two phase heat transfer coefficient gradually diminishes with increase in the gas and liquid flow rates (or Re_{SG} and Re_{SL}). For instance, at Re_{SL} = 6000 (0º $\leq \theta \leq$ -30º), the highest and average decrease in h_{TP} are 11% and 3% as compared to 47% and 30% for Re_{SL} = 2500. For low gas and liquid flow rates, stratified flow pattern prevails in downward pipe inclinations. As mentioned earlier, the physical structure of stratified flow patterns in downward pipe inclinations is such that there is no coupling between the two phases and dominant buoyancy forces act on the gas phase flowing on top of the liquid phase. The effect of buoyancy on the gas phase retards its motion, increases its residence time in the test section and as a result decreases the two phase heat transfer coefficient. For low gas and liquid Reynolds numbers, increase in h_{TP} for steeper pipe orientations could be explained based on the variation in the stratified flow pattern structure. For these near vertical and vertical downward pipe orientations (θ = -75º and -90º), the flow pattern is stratified and falling film flow, respectively. At -75º of pipe orientation, the visual observations show that the gas-liquid interface of stratified flow pattern is unstable such that the liquid phase splashes on the pipe top wall and momentarily bridges the pipe cross section. Barnea et al. (1982) also reported that at steeper pipe orientations, liquid lumps are torn away from the unstable gas-liquid interface all the way to the top wall of the pipe. They also mentioned that at low to moderate liquid flow rates, the gas-liquid interface in steeper pipe orientations tend to become concave and the liquid film climbs the tube periphery with increase in the liquid flow rate and pipe

orientation. This implies that, compared to near horizontal downward pipe inclinations, a greater fraction of the pipe circumference (wetted perimeter) is in contact with the liquid phase for near vertical downward pipe inclinations and hence permits higher rates of two phase heat transfer. For vertical downward flow, the entire pipe circumference is in contact with a thin liquid film and compared to the stratified flow structure, an axisymmetric thin liquid film allows higher heat transfer rates and hence higher values of two phase heat transfer coefficient. The three different forms of stratified flow with variation in the liquid film thickness and its circumferential distribution as a function of pipe orientation are depicted in Figure 4.5.

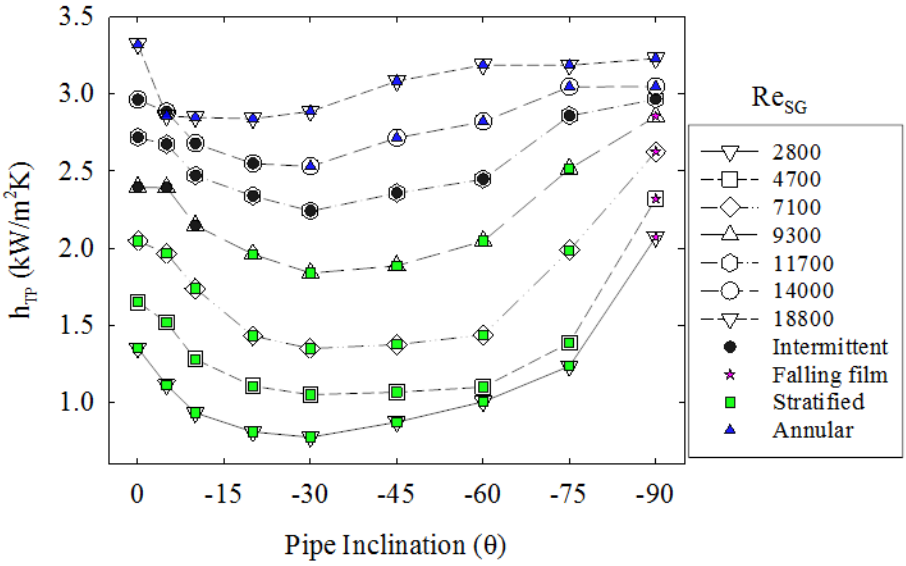

(a) Re_{SL} = 2500

Figure 4.4 (Continued on the next page)

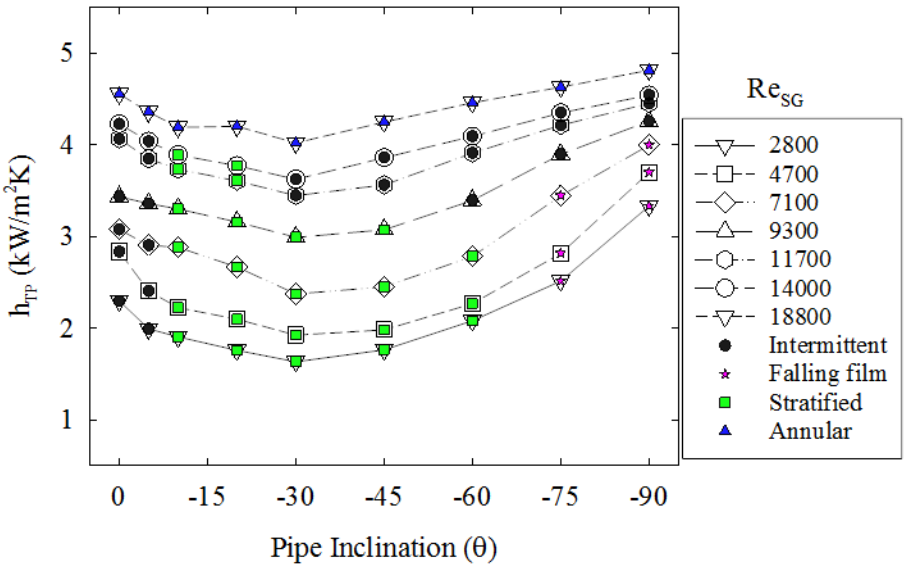

(b) Re_{SL} = 4000

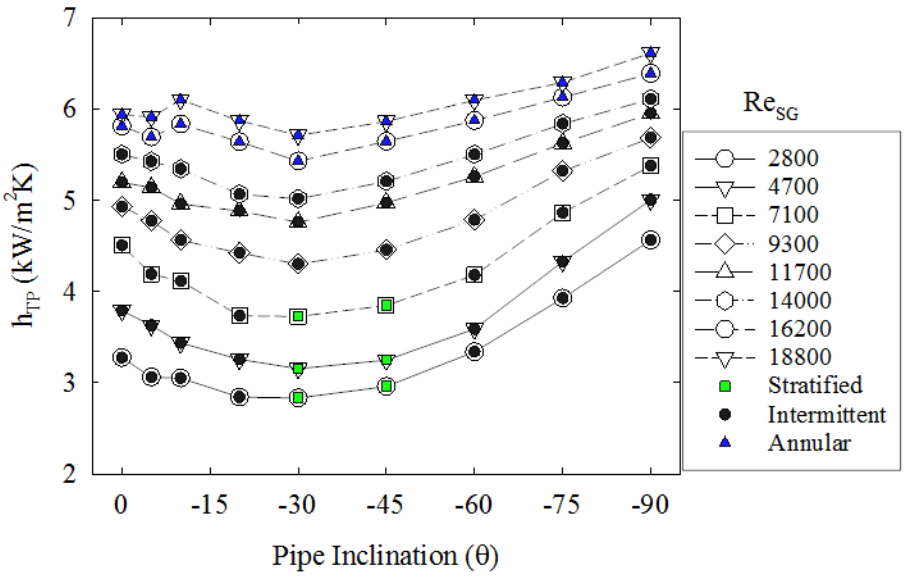

(c) Re_{SL} = 6000

Figure 4.4 Effect of pipe orientation on h_{TP} for fixed Re_{SL} and varying Re_{SG}

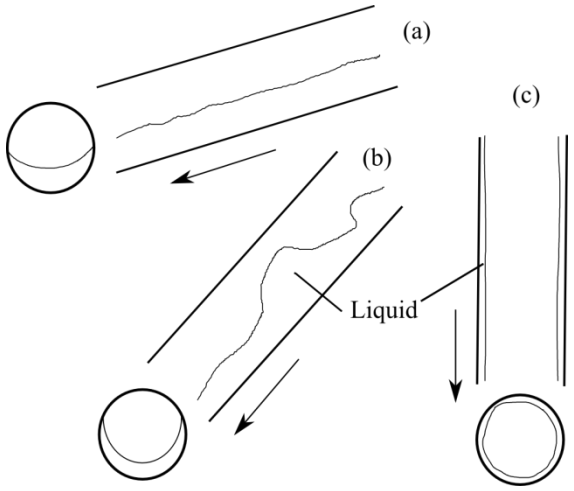

Figure 4.5 Variation in the liquid film thickness with change in pipe orientation (a) Near horizontal downward (b) Near vertical downward (c) Vertical downward (John et al. (2015))

In addition to the effect of pipe orientation, it is also of interest to check the parity between two phase heat transfer coefficients with single phase heat transfer coefficient measured at equivalent liquid flow rates. The single phase heat transfer coefficient h_L is calculated assuming only G (1-x) amount of liquid mass flows through the pipe occupying the entire pipe cross section. The single phase superficial liquid Reynolds number using this mass flux is then used to calculate h_L using Sieder and Tate (1936) correlation. As shown in Figure 4.6 (a), for low Re_{SL} and Re_{SG}, the ratio of h_{TP} to h_L changes considerably with change in downward pipe inclinations. Starting with the two phase flow in horizontal direction, increase in downward inclination initially decreases the h_{TP}/h_L ratio. In the vicinity of -30^o, this ratio is slightly less than unity meaning that the single phase heat transfer coefficients at equivalent liquid flow rates would be equal or greater than that in two phase flow. If the pipe is further inclined at steeper angles beyond -30^o then h_{TP}/h_L ratio increases gradually and a maximum amount of heat transfer in two phase flow with reference to that in single phase flow is obtained for vertical downward pipe orientation. This trend also implies that the two phase flow in near horizontal downward inclined stratified flow regime operating at low gas and liquid flow rates is an undesirable region that decreases the amount of heat transfer and the use of single phase flow may

yield better heat transfer. The maximum amount of two phase heat transfer at low gas and liquid flow rates (compared to single phase flow) also justifies the wide use of vertical downward sloping evaporators in several industrial applications to enhance the heat transfer rates with minimum pressure drop penalty factor. With increase in gas and liquid flow rates (or Re_{SG} and Re_{SL}), the ratio h_{TP}/h_L increases and is always greater than unity. However, with increase in downward pipe inclinations from horizontal this ratio is found to decrease consistently with a minimum in the vicinity of -30°. Thus it is evident that, irrespective of the gas and liquid flow rates and the entire range of downward pipe inclinations, the higher amount of two phase heat transfer is achieved either in horizontal or near vertical two phase flow.

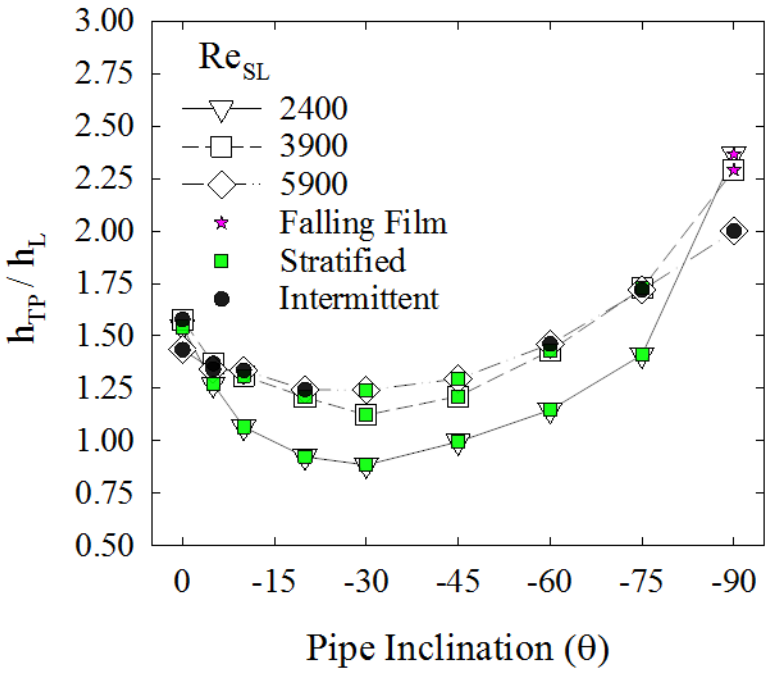

(a) Re_{SG} = 2800

Figure 4.6 (Continued on the next page)

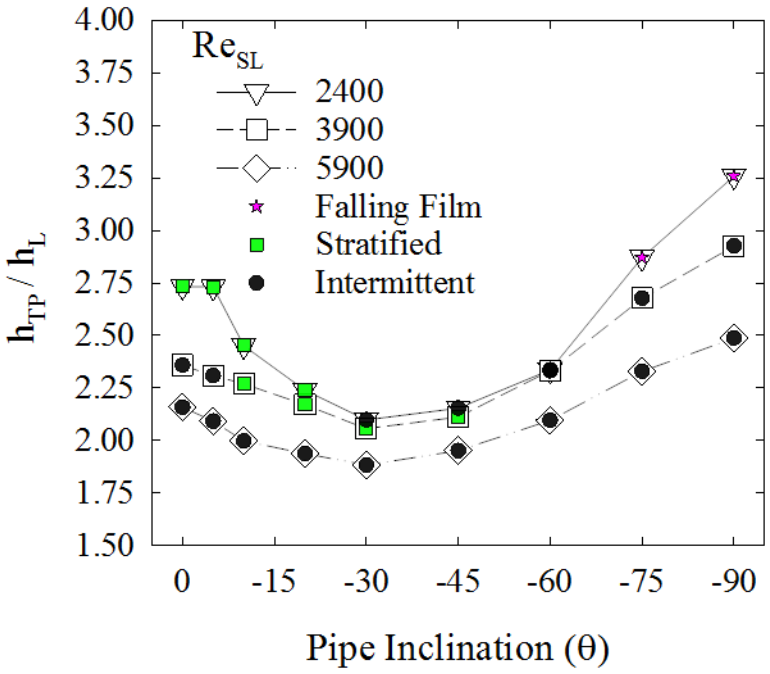

(b) Re_{SG} = 9300

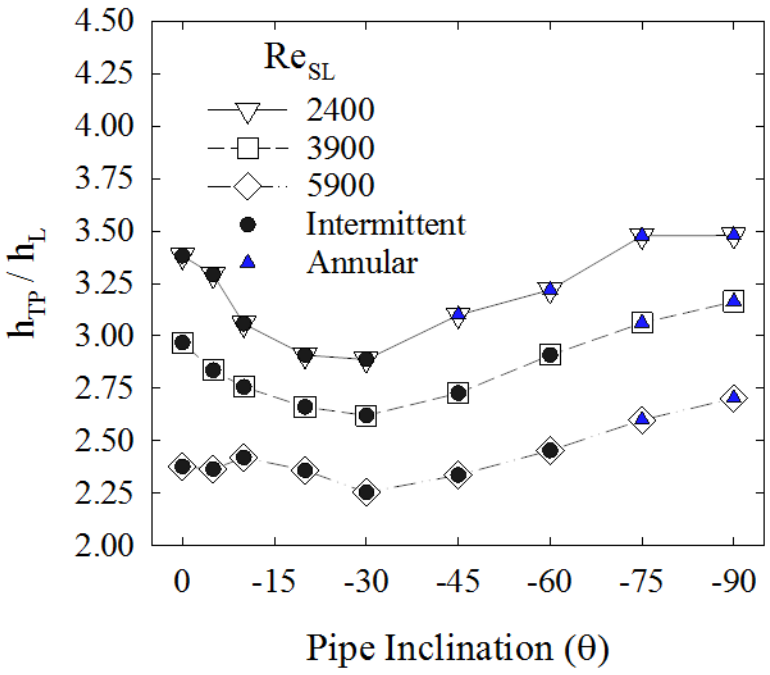

(c) Re_{SG} = 14000

Figure 4.6 Ratio of two phase to single phase heat transfer coefficient for varying flow patterns and pipe orientations

4.2.3 Analysis of Heat Transfer Correlations Performance

As mentioned earlier, the two phase literature provides several correlations to predict non-boiling two phase heat transfer coefficient. However, these correlations are mostly developed and validated against data in horizontal and vertical upward pipe orientations and their accuracy for downward inclined two phase flow is not known. Thus, it is of interest to check the performance of these existing correlations against the experimental data collected in this study. Based on the recommendations of Tang (2011), Hossainy (2014), and our preliminary analysis, the correlations selected and listed in Table 4.1 are compared against the experimental data. The criterion used for evaluating the performance of these correlations is based on the percentage of data points predicted within ±20% and ±30% error bands. Also, the overall performance of these correlations for the entire data is analyzed using statistical parameters such as mean absolute error and standard deviation given by Equations (4.3) and (4.4), respectively. The performance of a correlation is considered satisfactory if at least 70% and 80% of the data points are predicted within ±20% and ±30% error bands, respectively. It is shown in Figures 4.2 and 4.4 that the two phase heat transfer coefficient undergoes decreasing and increasing trends as the pipe is oriented from 0^o to -90^o. Hence, to get a better idea of the performance of different correlations over a narrow range of two phase flow conditions, their performance is checked against four ranges of pipe inclinations given as: "Horizontal and Near Horizontal Pipe Inclinations ($0^o \le \theta < -30^o$)", Mid-Range Pipe Inclinations ($-30^o \le \theta \le -60^o$)", "Vertical and Near Vertical Pipe Inclinations ($-60^o < \theta \le -90^o$)", and Overall Pipe Inclinations ($0^o \le \theta \le -90^o$).

$$\text{Absolute mean error} = \frac{1}{N}\sum_{j=1}^{N}\left|\varepsilon_j\right| \tag{4.3}$$

$$\text{Where } \left|\varepsilon_j\right| = \left|\frac{h_{TP,cal} - h_{TP,\exp}}{h_{TP,\exp}}\right| \tag{4.3a}$$

$$\%\,\text{Std. deviation} = \sqrt{\frac{1}{N-1}\sum_{j=1}^{N}\left(\varepsilon_j - \bar{\varepsilon}\right)^2} \times 100 \tag{4.4}$$

Table 4.1 List of selected correlations for heat transfer data analysis

Sources	Correlations
Aggour (1978)	$h_{TP} = h_L(1-\alpha)^{-0.33}$ (Laminar) and $h_{TP} = h_L(1-\alpha)^{-0.83}$ (Turbulent)
Chu and Jones(1980)	$h_{TP} = 0.47\left(\mathrm{Re}_{SL}/(1-\alpha)\right)^{0.55}\mathrm{Pr}_L^{0.33}\left(\mu_b/\mu_w\right)^{0.14}(P_a/P_{sys})^{0.17}\left(k_L/D_i\right)$
Khoze et al. (1976)	$Nu_{TP} = 0.26\left(\mathrm{Re}_{SG}\right)^{0.2}\left(\mathrm{Re}_{SL}\right)^{0.55}\mathrm{Pr}_L^{0.4}$
Kim and Ghajar (2006)[1]	$h_{TP} = h_L \times F_p\left(1+0.7\left[\left(\frac{x}{1-x}\right)^{0.08}\left(\frac{1-F_p}{F_p}\right)^{0.06}\left(\frac{\mathrm{Pr}_G}{\mathrm{Pr}_L}\right)^{0.03}\left(\frac{\mu_G}{\mu_L}\right)^{-0.14}\right]\right)$ $F_p = (1-\alpha)+\alpha\left[\left(\frac{2}{\pi}\tan^{-1}\sqrt{\frac{\rho_G(V_G-V_L)^2}{gD_i(\rho_L-\rho_G)}}\right)^2\right];\ V_G = \frac{V_{SG}}{\alpha}\ \text{and}\ V_L = \frac{V_{SL}}{1-\alpha}$
Knott et al. (1959)	$h_{TP} = h_L \times \left(1+V_{SG}/V_{SL}\right)^{0.33}$
Martin and Sims (1971)	$h_{TP} = h_L \times \left(1+0.64\sqrt{V_{SG}/V_{SL}}\right)$
Oshinowo et al. (1984)	$Nu_{TP} = 1.2\left(\mathrm{Re}_{SL}\right)^{0.6}\mathrm{Pr}_L^{1/3}\left(\mu_b/\mu_w\right)^{0.14}\left(\mu_G/\mu_L\right)^{0.2}\left(V_{SG}/V_{SL}\right)^{0.1}$
Ravipudi and Godbold (1978)	$Nu_{TP} = 0.56\left(\mathrm{Re}_{SL}\right)^{0.6}\mathrm{Pr}_L^{0.33}\left(\mu_b/\mu_w\right)^{0.14}\left(\mu_G/\mu_L\right)^{0.2}\left(V_{SG}/V_{SL}\right)^{0.3}$
Rezkallah and Sims (1987)	$h_{TP} = h_L(1-\alpha)^{-0.9}$
Shah (1981)[2]	$h_{TP} = h_L \times \left(1+V_{SG}/V_{SL}\right)^{0.25}$
Tang and Ghajar (2007)[3]	$h_{TP} = h_L \times F_p\left(1+0.55\left[\left(\frac{x}{1-x}\right)^{0.1}\left(\frac{1-F_p}{F_p}\right)^{0.4}\left(\frac{\mathrm{Pr}_G}{\mathrm{Pr}_L}\right)^{0.25}\left(\frac{\mu_L}{\mu_w}\right)^{0.25} I^{0.25}\right]\right)$ $F_p = (1-\alpha)+\alpha\left[\left(\frac{2}{\pi}\tan^{-1}\sqrt{\frac{\rho_G(V_G-V_L)^2}{gD_i(\rho_L-\rho_G)}}\right)^2\right];\ V_G = \frac{V_{SG}}{\alpha}\ \text{and}\ V_L = \frac{V_{SL}}{1-\alpha}$ $I = 1+\frac{(\rho_L-\rho_G)gD_i^2\lvert\sin\theta\rvert}{\sigma}$

[1]Use Chisholm (1973) correlation to calculate void fraction, [2] For Shah (1981) consider turbulent flow if $Re_{SL} > 170$, [3]Use Chisholm (1973) correlation to calculate void fraction, h_L is based on Sieder and Tate (1936) with Re_{SL} replaced by $Re_L = Re_{SL}/(1-\alpha)^{0.5}$ required in F_p.

I. Horizontal and Near Horizontal Pipe Inclinations ($0° \leq \theta < -30°$)

As shown in Table 4.2, for horizontal and near horizontal downward inclined pipe orientations, the correlation of Shah (1981) gives the best performance by predicting 77% and 85% of data points within ±20% and ±30% error bands, respectively. For stratified flow regime, no correlation under consideration is able to perform satisfactorily. In comparison to all other correlations for stratified flow regime, Kim and Ghajar (2006) and Tang and Ghajar (2007) show relatively good performance and predict 72% and 62% of data points within ±30% error bands, respectively. Shah (1981) correlation predicts 85% and 95% of data points within ±30% error bands for slug and intermittent flow patterns, respectively. The correlation of Tang and Ghajar (2007) gives satisfactory performance in slug flow regime by predicting 70% and 83% of data points within ±20% and ±30% error bands, respectively. Its accuracy is found to decrease in intermittent flow regime. Note that the correlation of Tang and Ghajar (2007) is developed based on the experimental data for horizontal and upward pipe inclinations. Moreover, majority of the experimental data used to fix the empirical parameters in their correlation consisted of non-intermittent flow patterns which might be a reason why Tang and Ghajar (2007) correlation does not perform satisfactorily in intermittent flow regime. Nevertheless, their correlation still predicts more than 74% of data points within ±30% error bands for the pipe orientation range analyzed in this section. It is important to note that the correlation of Khoze et al. (1976) and Oshinowo et al. (1984) performed very poorly as they failed to predict any data points in the pipe orientation range analyzed in this section. It is also found that most of the correlations listed in Table 4.2 give higher accuracy when analyzed only against the horizontal two phase flow data. This clearly indicates that these correlations over predict the two phase heat transfer coefficient in near horizontal downward pipe inclination. For this pipe orientation range ($0^o \leq \theta < -30^o$), Shah (1981) correlation is recommended.

Table 4.2 Performance of non-boiling two phase heat transfer correlations for $0^o \leq \theta < -30^o$

Flow patterns	All flow patterns				Stratified		Slug		Intermittent/Annular	
No. of data points	337				55		60		222	
Correlations	(1)	(2)	(3)	(4)	(1)	(2)	(1)	(2)	(1)	(2)
Aggour (1978)	74	83	20	30	22	22	75	88	88	97
Chu and Jones (1980)	16	31	76	88	0	0	0	2	24	47
Khoze et al. (1976)	0	0	339	286	0	0	0	0	0	0
Kim and Ghajar (2006)	64	73	26	71	67	72	0	5	81	92
Knott et al. (1959)	38	55	40	40	0	2	55	72	42	64
Martin and Sims (1971)	5	11	89	72	24	29	80	92	69	94
Oshinowo et al. (1984)	0	0	191	170	0	0	0	0	0	0
Ravipudi and Godbold (1978)	11	17	96	100	0	0	43	52	13	21
Rezkallah and Sims (1987)	63	83	22	28	33	53	27	48	11	21
Shah (1981)	77	85	22	36	36	45	75	85	87	95
Tang and Ghajar (2007)	52	74	24	23	52	62	70	83	47	74

(1) % of data points predicted within ±20% error bands, (2) % of data points predicted within ±30% error bands, (3) % mean absolute error and (4) standard deviation.

II. Mid-Range Pipe Inclinations ($-30° \leq \theta \leq -60°$)

For the mid-range pipe orientations, Table 4.3 shows that the correlations of Shah (1981) and Tang and Ghajar (2007) are the top performing correlations for all flow patterns and pipe inclinations considered in this section. Shah (1981) and Tang and Ghajar (2007) correlations predict 69% and 74%, and 71% and 79% of data points within ±20% and ±30% error bands, respectively for all flow patterns. In the stratified flow regime, none of the correlations listed in Table 4.3 give satisfactory performance. In the slug flow regime, Shah (1981) and Tang and Ghajar (2007) predict 100% and 95% of data points within ±30% error bands, respectively. Also, Knott et al. (1959) and Rezkallah

and Sims (1987) predict 100% of data points within ±30% in this regime. In the intermittent flow, Shah (1981), Rezkallah and Sims (1987), and Tang and Ghajar (2007) predict 97%, 93%, and 96% of data points within ±30% error bands, respectively. In the annular flow regime, Tang and Ghajar (2007) predicts 100% of data points within ±30% error bands.

Table 4.3 Performance of non-boiling two phase heat transfer correlations for $-30^{o} \leq \theta \leq -60^{o}$

Flow patterns	All flow patterns				Stratified		Slug		Intermittent		Annular	
No. of data points	255				75		22		131		27	
Correlations	(1)	(2)	(3)	(4)	(1)	(2)	(1)	(2)	(1)	(2)	(1)	(2)
Aggour (1978)	65	75	30	40	25	33	100	100	84	95	48	67
Chu and Jones (1980)	21	32	93	107	0	0	0	5	22	30	22	30
Khoze et al. (1976)	0	0	377	329	0	0	0	0	0	0	0	0
Kim and Ghajar (2006)	60	73	31	99	32	45	0	0	84	97	70	92
Knott et al. (1959)	40	50	56	68	5	9	95	100	53	67	22	33
Martin and Sims (1971)	5	13	112	99	0	1	50	86	1	9	0	0
Oshinowo et al. (1984)	0	0	223	204	0	0	0	0	0	0	0	0
Ravipudi and Godbold (1978)	14	20	125	133	3	4	72	95	13	21	0	0
Rezkallah and Sims (1987)	53	74	32	36	32	37	100	100	59	93	46	58
Shah (1981)	69	74	32	48	19	21	100	100	92	97	70	81
Tang and Ghajar (2007)	71	79	27	50	27	39	91	95	94	96	70	100

(1) % of data points predicted within ±20% error bands, (2) % of data points predicted within ±30% error bands, (3) % mean absolute error and (4) standard deviation.

The accuracy of Knott et al. (1959) and Aggour (1978) correlations are found to decrease with change in flow pattern from slug to intermittent and then from intermittent to annular flow regime. Some of the worst performing correlations are those of Khoze et al. (1976) and Oshinowo et al. (1984). These correlations fail to predict any data points in the mid-range pipe inclination.

Considering the entire data for this range of pipe orientations, Tang and Ghajar (2007) is identified as the best performing correlation capable of predicting 79% of data points within ±30% error bands. The drop in overall accuracy is essentially due to inaccurate prediction in stratified flow regime. Tang and Ghajar (2007) is recommended for $-30^{o} \leq \theta \leq -60^{o}$ pipe orientation range.

III. Vertical and Near Vertical Pipe Inclinations ($-60° < \theta \leq -90°$)

For vertical and near vertical pipe orientations, Table 4.4 shows that Shah (1981) correlation is the best performing correlation since it predicts 96% of data points within ±30% error bands. Also, the correlations of Martin and Sims (1971), Knott et al. (1959) and Tang and Ghajar (2007) perform satisfactorily and are the best performing correlations for slug, intermittent and annular flow patterns, respectively. For the combined stratified and falling film flow patterns, the correlation of Shah (1981) gives best accuracy by predicting 83% of data points within ±30% error bands. Although, for all flow patterns combined together, Knott et al. (1959) correlation gives highest accuracy within ±20% error bands, these numbers are biased towards high number of data points in intermittent flow regime. In fact, Shah (1981) and Tang and Ghajar (2007) correlations perform much better than Knott et al. (1959) correlation in stratified+falling film flow (83% and 73% of data within ±30% error bands, respectively) and annular flow (100% of data within ±30% error bands) patterns, respectively. Overall, for $-60° < \theta \leq -90°$ Shah (1981) correlation is recommended since it gives the best performance for all flow patterns in this pipe orientation range.

Table 4.4 Performance of non-boiling two phase heat transfer correlations for $-60^o < \theta \leq -90^o$

Flow patterns	All flow patterns				Slug		Intermittent		Stratified + falling film		Annular	
No. of data points	152				28		65		35		24	
Correlations	(1)	(2)	(3)	(4)	(1)	(2)	(1)	(2)	(1)	(2)	(1)	(2)
Aggour (1978)	30	62	23	13	57	89	17	66	54	71	42	75
Chu and Jones (1980)	40	43	47	47	36	39	77	82	0	0	50	50
Khoze et al. (1976)	0	0	257	266	0	0	0	0	0	0	0	0
Kim and Ghajar (2006)	34	69	24	25	46	71	14	60	34	66	75	100
Knott et al. (1959)	74	80	21	26	93	100	89	92	43	46	61	74
Martin and Sims (1971)	31	43	52	71	100	100	23	49	9	11	4	8
Oshinowo et al. (1984)	0	0	127	141	0	0	0	0	0	0	0	0
Ravipudi and Godbold (1978)	28	39	65	92	89	100	28	48	0	0	4	4
Rezkallah and Sims (1987)	18	39	28	13	25	64	9	29	43	63	38	58
Shah (1981)	57	96	19	14	57	100	48	100	69	83	67	100
Tang and Ghajar (2007)	34	68	19	10	79	96	22	74	46	77	83	100

(1) % of data points predicted within ±20% error bands, (2) % of data points predicted within ±30% error bands, (3) % mean absolute error and (4) standard deviation.

IV. Overall Pipe Inclinations ($0° \leq \theta \leq -90°$)

For the entire data (all flow patterns and pipe orientations), Table 4.5 shows that the correlation of Shah (1981) is relatively the best performing correlation since it predicts 83% of data points within ±30% error bands. For slug and intermittent flow patterns, his correlation predicts more than 90% of data points within ±30% error bands whereas for annular flow regime, Tang and Ghajar (2007) is the best performing correlation that predicts 100% of data points within ±30% error bands. For slug flow, most of the correlations give satisfactory performance by predicting at least 70% and 80% of data points within ±20% and ±30% error bands, respectively. For intermittent flow regime, Shah (1981) and Aggour (1978) correlations predict 96% and 92% of data points within ±30% error bands,

respectively. Note that none of these correlations perform satisfactorily in stratified flow regime. Considering the overall predictions, correlation of Shah (1981) appears to give the best accuracy in comparison to other correlations and hence is recommended for use against all flow patterns except for the stratified flow in downward pipe inclinations. Tang and Ghajar (2007) correlation may be used in annular flow to achieve a better accuracy.

Table 4.5 Performance of non-boiling two phase heat transfer correlations for $0^o \leq \theta \leq -90^o$

Flow patterns	All flow patterns				Stratified + falling film		Slug		Intermittent		Annular	
No. of data points	744				165		110		418		51	
Correlations	(1)	(2)	(3)	(4)	(1)	(2)	(1)	(2)	(1)	(2)	(1)	(2)
Aggour (1978)	62	76	24	73	30	37	75	90	76	92	45	71
Chu and Jones (1980)	23	34	75	92	0	0	9	12	32	47	35	39
Khoze et al. (1976)	0	0	335	294	0	0	0	0	0	0	0	0
Kim and Ghajar (2006)	52	72	27	74	44	58	12	21	72	89	72	96
Knott et al. (1959)	59	67	41	55	11	15	73	85	53	69	40	52
Martin and Sims (1971)	10	18	89	82	2	3	49	59	4	15	2	4
Oshinowo et al. (1984)	0	0	189	176	0	0	0	0	0	0	0	0
Ravipudi and Godbold (1978)	15	23	100	110	1	2	61	73	15	25	2	2
Rezkallah and Sims (1987)	50	71	27	69	32	40	70	86	57	84	42	58
Shah (1981)	70	83	25	38	34	42	75	92	83	96	69	90
Tang and Ghajar (2007)	55	74	24	74	39	55	76	89	58	81	76	100

(1) % of data points predicted within ±20% error bands, (2) % of data points predicted within ±30% error bands, (3) % mean absolute error and (4) standard deviation.

The plot of h_{TP} predicted by Shah (1981) correlation against measured h_{TP} for $0^o \leq \theta \leq -90^o$ pipe orientation for intermittent flow regime is shown in Figure 4.7. It is noted from this plot that about 96% of the data points fall within ±30% error bands. Also, Figure 4.8 shows the plot of h_{TP}

predicted by Shah (1981) correlation against measured h_{TP} for $0^o \leq \theta \leq -90^o$ for all flow patterns except stratified flow. Also, Figure 4.9 shows the plot of h_{TP} predicted by Shah (1981) correlation against measured h_{TP} for only stratified flow pattern. It can be seen from this plot that only about 36% of data points fall within ±30% error bands. This implies that some adjustment can be made to enhance the performance of Shah (1981) correlation for downward pipe orientation in stratified flow regime. A factor that accounts for the effect of flow pattern has been introduced to enhance the overall performance of Shah (1981) correlation for downward pipe orientation. This is explained in detail in the next section.

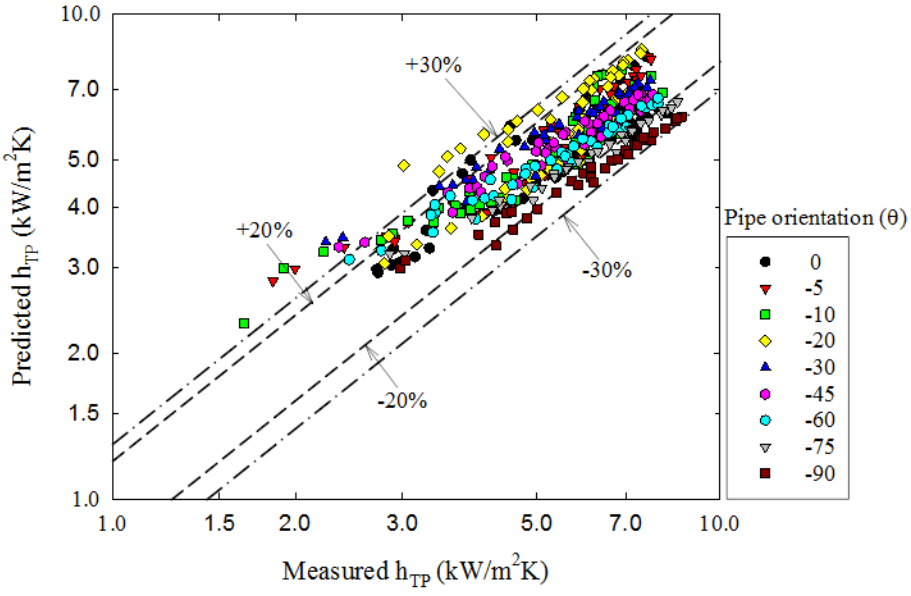

Figure 4.7 Performance of Shah (1981) correlation for $0^o \leq \theta \leq -90^o$ (Intermittent flow)

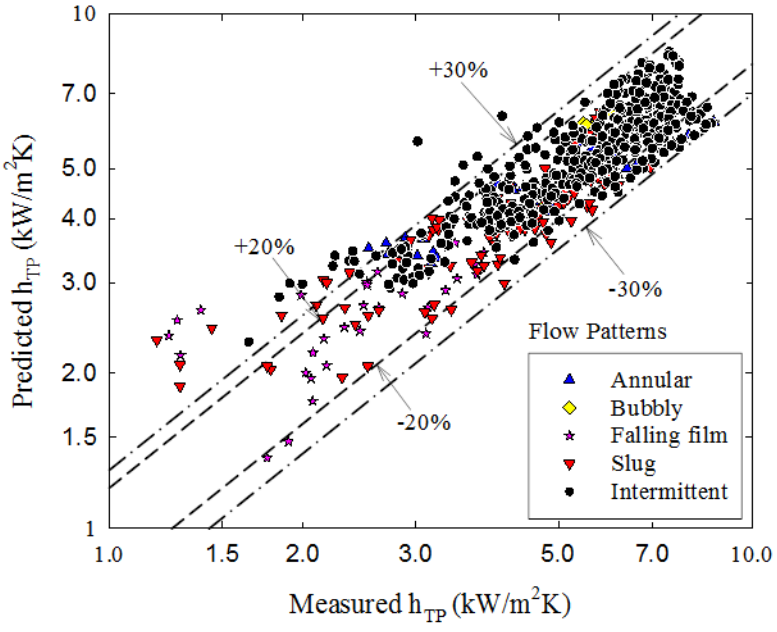

Figure 4.8 Performance of Shah (1981) correlation for all flow patterns except stratified flow pattern

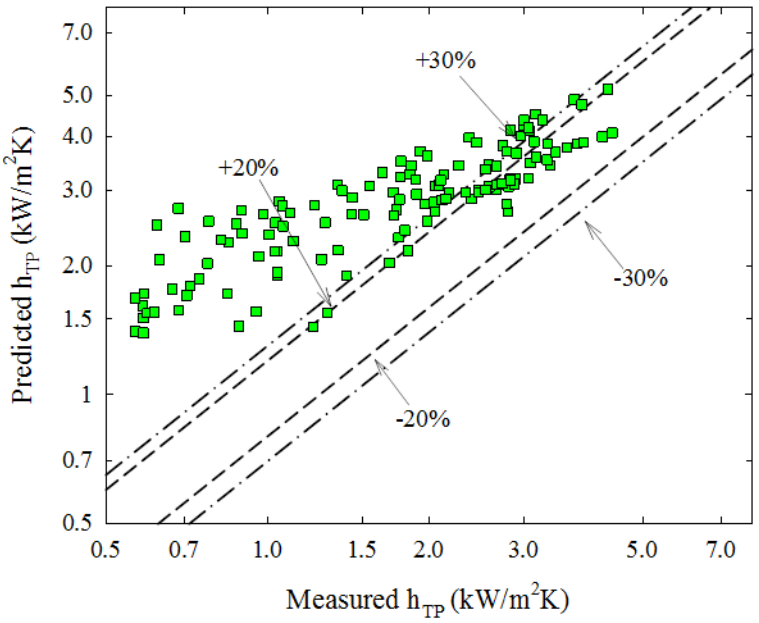

Figure 4.9 Performance of Shah (1981) correlation for stratified flow pattern

4.2.4 Correlation Development

From the analysis in the previous section, it is evident that the performance of these correlations depend on both flow patterns and pipe inclination. Shah (1981) correlation is the best performing correlation for all flow patterns and pipe inclinations analyzed in this work, but it only predicts 70% and 83% of the data points within ±20% and ±30% error bands, respectively. This suggests that there is potential for improvement of this correlation. An enhanced performance of Shah (1981) correlation can be achieved by introducing a new factor that will account for the effect of flow pattern for downward two phase heat transfer, and adjusting the exponent in order to increase the overall performance of the correlation.

From Tables 4.2 and 4.3, it is evident that Shah (1981) correlation fails to perform satisfactorily in $0^o \leq \theta < -30^o$ and $-30^o \leq \theta \leq -60^o$ pipe inclinations. For $0^o \leq \theta < -30^o$ pipe inclinations, it only predicts 45% of stratified flow data points within ±30% error bands. Also, for $-30^o \leq \theta \leq -60^o$ pipe inclinations, it only predicts 21% and 81% of stratified and annular flow data points, respectively within ±30% error bands. In order to enhance the performance of Shah (1981) correlation in these flow regimes thereby increasing the overall performance of Shah (1981) correlation, a flow pattern factor, F_P, introduced by Kim and Ghajar (2006) has been adopted. They developed a parameter to represent flow patterns in two phase flow which is the square of the ratio of the effective wetted perimeter to the circumference of a circular pipe.

Considering the effect of void fraction, inertia and gravity forces in the two phase flow, the flow pattern factor becomes:

$$F_p = (1-\alpha) + F_s^2\alpha \tag{4.5}$$

Where,

$$F_s = \frac{2}{\pi}\left(\tan^{-1}\sqrt{\frac{\rho_G (V_G - V_L)^2}{gD(\rho_L - \rho_G)}}\right) \tag{4.6}$$

F_S is called the shape factor. This shape factor represents the change in the shape of gas-liquid interface due to the effect of momentum and gravity force. Also, α is calculated from Chisholm (1973). The new proposed correlation is given as:

$$\frac{h_{TP}}{h_L} = (1 + \frac{V_{SG}}{V_{SL}})^{\frac{1}{4}} \quad F_p{}^p \tag{4.7}$$

For 0º ≤ θ < -30º and -30º ≤ θ ≤ -60º pipe inclinations, the best suitable exponent (p) is found to be 0.2. Table 4.6 shows the comparison of performance of Shah (1981) correlation and the proposed correlation. For 0º ≤ θ < -30º pipe inclinations, in the stratified flow regime, the proposed correlation predicts 70% of data points within ±30% error bands compared to Shah (1981) correlation which predicts only 45%. Also, in the slug flow regime, the proposed correlation predicts 92% of data points within ±30% error bands compared to Shah (1981) correlation which predicts only 85%. Finally, for all flow patterns in the 0º ≤ θ < -30º pipe inclinations, the proposed correlation predicts 91% of data points within ±30% error bands compared to Shah (1981) correlation which predicts only 85%. For 30º ≤ θ ≤ -60º pipe inclinations, in the annular flow regime, the proposed correlation predicts 100% of data points within ±30% error bands compared to Shah (1981) correlation which predicts only 81%. Overall, for all flow patterns in 30º ≤ θ ≤ -60º pipe inclinations, the proposed correlation predicts 83% of data points within ±30% error bands compared to Shah (1981) correlation which predicts only 74%. For all flow patterns and pipe inclinations (0º ≤ θ ≤ -90º), the proposed correlation predicts 90% of data points within ±30% error bands compared to Shah (1981) correlation which predicts only 83%. Figure 4.10 shows the plot of h_{TP} predicted by the proposed correlation against measured h_{TP} for 0º ≤ θ ≤ -90º pipe inclinations for all flow patterns except stratified flow. It is evident from this plot that for slug, intermittent, and annular flow the proposed correlation predicts at least 96% of the data points within ±30% error bands. It is pertinent to note that for the stratified flow regime, despite slight improvement

given by the proposed correlation, there is still need to develop a separate correlation for this flow regime.

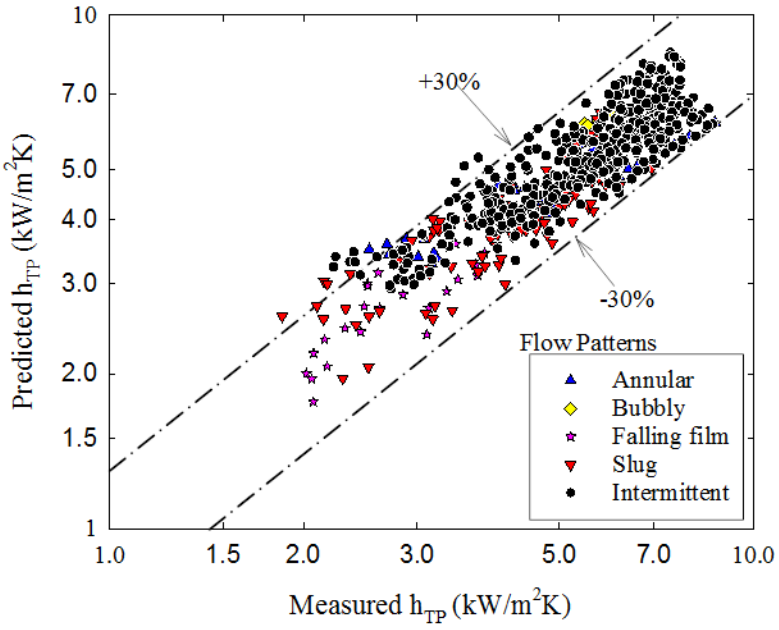

Figure 4.10 Performance of proposed correlation for all flow patterns except stratified flow pattern

Table 4.6 Comparison of performance of Shah (1981) correlation and proposed correlation

Flow patterns	All flow patterns				Stratified/Falling Film		Slug		Intermittent /Annular		Annular	
Correlations	(1)	(2)	(3)	(4)	(1)	(2)	(1)	(2)	(1)	(2)	(1)	(2)
No. of data points ($0^o \leq \theta < -30^o$)	337				55		60		222		-	
Shah (1981)	77	85	22	36	36	45	75	85	87	95	-	-
Proposed Correlation (use p = 0.2 in Equation 4.7)	67	91	19	25	62	70	80	92	84	96		
No. of data points ($-30^o \leq \theta \leq -60^o$)	255				75		22		131		27	
Shah (1981)	69	74	32	48	19	21	100	100	92	97	70	81
Proposed Correlation (use p = 0.2 in Equation 4.7)	61	83	26	30	39	43	100	100	93	100	78	100
No. of data points ($-60^o < \theta \leq -90^o$)	152				35		28		65		24	
Shah (1981)	57	96	19	14	63	83	57	100	48	100	67	100
Proposed Correlation (use p = 0 in Equation 4.7)	57	96	19	14	63	83	57	100	48	100	67	100
No. of data points ($0^o \leq \theta \leq -90^o$)	744				165		110		418		51	
Shah (1981)	70	83	25	38	34	42	75	92	83	96	69	90
Proposed Correlation	63	90	21	73	52	60	83	96	81	98	73	100

(1) % of data points predicted within ±20% error bands, (2) % of data points predicted within ±30% error bands, (3) % mean absolute error and (4) standard deviation.

CHAPTER V

CONCLUSIONS AND RECOMMENDATIONS

In this study, non-boiling heat transfer two phase flow for downward pipe orientation is investigated. Experiments were carried out to measure the local and averaged non-boiling two phase heat transfer coefficient (h_{TP}) in 0, -5, -10, -20, -30, -45, -60, -75 and -90 degrees of pipe inclinations. The experiments were carried out with uniform wall heat flux boundary condition in 12.5 mm I.D. stainless steel pipe that uses air-water as fluid combination and consists of all flow patterns that covers the gas and liquid superficial Reynolds numbers in a range of 270 to 19000 and 2300 to 17000, respectively. It is observed that an increase in downward pipe inclination from horizontal initially exhibits a decreasing tendency of h_{TP} till -30 degrees and thereafter increases consistently with further increase in the pipe inclination towards vertical downward direction. The measured data is compared against some of the relevant non-boiling two phase heat transfer correlations available in the two phase flow literature. The summary of this work and future recommendations are presented in this chapter

5.1 Conclusion of Results

1) The experimental data shows dependency of two phase heat transfer coefficient on both flow patterns and pipe orientation. For a fixed pipe orientation and low liquid flow rates,

the two phase heat transfer coefficient is relatively insensitive to change in gas flow rates in slug and stratified flow regimes. It increases rapidly in intermittent and annular regime owing to the turbulent nature of these flow patterns marked by vigorous mixing and interaction between gas-liquid interface and disturbance waves.

2) At low liquid and low to moderate gas flow rates, the two phase heat transfer coefficient decreases rapidly (with a minimum around -30^o to -45^o) as the pipe is orientated from horizontal to downward pipe inclinations. For a fixed flow pattern and phase flow rates, highest h_{TP} is found for near vertical pipe orientations. The flow physics that causes this increase in h_{TP} compared to other pipe orientations especially in slug and stratified flow patterns is justified considering the variation in physical structure of the flow patterns.

3) The two phase heat transfer coefficient is found to be less than single phase heat transfer coefficient at low gas and liquid flow rates in near horizontal downward pipe inclinations specifically at -30^o and hence this region of two phase flow may be regarded as an undesirable region for practical applications requiring enhanced heat transfer rates.

4) The non-boiling two phase heat transfer correlations available in literature are compared with the measured values of h_{TP}. The comparisons are made for three different ranges of the pipe orientations and different flow patterns. The correlation of Shah (1981) is found to be the relatively best performing correlation for the entire data that predicts around 70% and 83% of data points within ±20% and ±30% error bands, respectively for all flow patterns. For annular flow pattern, Tang and Ghajar (2007) correlation is recommended for use since it performs better than Shah (1981) correlation.

5) Shah correlation is the best performing correlation for all flow patterns and pipe inclinations analyzed in this work, but it only predicts 70% and 83% of the data points within ±20% and

±30% error bands, respectively. This suggests that there is potential for improvement of this correlation. Hence, a more precise performance of Shah (1981) correlation is proposed. From Table 4.6, for all flow patterns in $0^o \leq \theta < -30^o$ pipe inclinations, the proposed correlation predicts 91% of data points within ±30% error bands compared to Shah (1981) correlation which predicts only 85%. For all flow patterns in $30^o \leq \theta \leq -60^o$ pipe inclinations, the proposed correlation predicts 83% of data points within ±30% error bands compared to Shah (1981) correlation which predicts only 73%. For all flow patterns and pipe inclinations ($0^o \leq \theta \leq -90^o$), the proposed correlation predicts 90% of data points within ±30% error bands as compared to Shah (1981) correlation which predicts only 83%.

5.2 Future Recommendations

1) Develop a new correlation specifically for stratified flow since existing correlations found in the literature fail to accurately predict heat transfer coefficient in stratified flow regime.

2) Incorporate the experimental results and analysis of Korivi et al. (2015) for upward pipe orientations ($0° \leq \theta \leq 90°$) and those presented in this study, and perform an overall analysis to cover the full range of pipe orientations ($-90° \leq \theta \leq 90°$).

3) Develop a new correlation based on the analysis in 2) that will be able to predict two phase heat transfer coefficient for the full range of pipe orientations ($-90° \leq \theta \leq 90°$).

REFERENCES

Aggour, M. A. (1978). Hydrodynamics and Heat Transfer in Two-Phase Two-Component Flow. (Ph.D. Dissertation), University of Manitoba, Canada.

Barnea, D., Shoham, O. and Taitel, Y. (1982). Flow Pattern Transition for Downward Inclined Two Phase Flow: Horizontal to Vertical, *Chemical Engineering Science,* 37, pp. 735-740.

Bhagwat, S. M., Mollamahmutoglu, M., & Ghajar, A. J. (2012). Experimental Investigation and Empirical Analysis of Non-Boiling Gas-Liquid Two Phase Heat Transfer in Vertical Downward Pipe Orientation. *Proceedings of ASME 2012 Summer Heat Transfer Conference (HT2012),* Puerto Rico, July 8-12.

Chisholm, D. (1973). Void Fraction During Two-Phase Flow. *J. Mechanical Engineering Science, 15*, 235-236.

Chu, Y. C., & Jones, B. G. (1980). Convective Heat Transfer Coefficient Studies in Upward and Downward Vertical Two-Phase Non-Boiling Flows. *AIChE., 7*, 79-90.

Cook, W. L. (2008). An Experimental Apparatus for Measurement of Pressure Drop, Void Fraction, and Non-Boiling Two-Phase Heat Transfer and Flow Visualization in Pipes for All Inclinations. (MS), Oklahoma State University, Stillwater.

Crawford, T. J. (1983). Analysis of Steady State and Transient Two Phase Flows in Downwardly Inclined Lines. (Ph.D), Drexel University.

Dittus, F. W. and Boelter, L. M. K. (1930). Heat Transfer Inautomobile Radiators of The Tubular Type. *University of California Publications in Engineering*, vol. 2, pp. 443-461.

Dorresteijn, W. R. (1970). Experimental Study of Heat Transfer in Upward and Downward Two Phase Flow of Air and Oil through 700 M Tubes. *Proccedings of the 4th International Heat Transfer Conference*.

Drucker, M. I., Dhir, V. K., & Duffey, R. B. (1984). Two Phase Heat Transfer for Flow in Tubes and over Rod Bundles with Blockages. *Trans. of ASME, J. of Heat Transfer*.

Ghajar, A. J., & Kim, J. (2006). *Calculation of Local inside-Wall Convective Heat Transfer Parameters from Measurements of the Local Outside-Wall Temperatures Along an Electrically Heated Circular Tube, Heat Transfer Calculations*. NewYork, NY: Mc-Graw-Hill.

Ghajar, A. J., & Tam, L. M. (1994). Heat Transfer Measurements and Correlations in the Transition Region for a Circular Tube with Three Different Inlet Configurations, Experimental Thermal and Fluid Science. *8*, 79-90.

Godbole P. V., Tang, C. C., & Ghajar, A. J. (2011). Comparison of void fraction correlations for different flow patterns in upward vertical two phase flow. *Heat Transfer Engineering*, 32 (10), 843–860.

Hossainy, T. A. (2014). Non-Boiling Heat Transfer in Horizontal and near Horizontal Downward Inclined Gas-Liquid Two Phase Flow. (MSc.), Oklahoma State University, Stillwater, Oklahoma.

Hossainy, T. A., Bhagwat, S. M., & Ghajar, A. J. (2014). Non-Boiling Heat Transfer in Horizontal and near Horizontal Downward Inclined Gas-Liquid Two Phase Flow. *10th International Conference on Heat Transfer, Fluid Mechanics and Thermodynamics*, Orlando, Florida.

John, T. J., Bhagwat, S. M., & Ghajar, A. J. (2015). Heat Transfer Measurement and Correlations Assessment for Downward Inclined Gas-Liquid Two Phase Flow. *Proceedings of the 1st Thermal and Fluid Engineering Summer Conference*, New York City, USA, August 9-12.

Khoze, A. N., Dunayev, S. V., & Sparin, V. A. (1976). Heat and Mass Transfer in Rising Two-Phase Flows in Rectangular Channels. *Heat Transfer - Soviet Research, 8*(3), 87-90.

Kim, J., & Ghajar, A. J. (2006). A General Heat Transfer Correlation for Non-Boiling Gas-Liquid Flow with Different Flow Patterns in Horizontal Pipes. *Int. J. Multiphase Flow, 32*, 447–465.

Kline, S. J., & McClintock, F. A. (1953). Describing Uncertainties in Single Sample Experiments. *Mechanical Engineering, 1*, 3-8.

Knott, R. F., Anderson, R. N., Acrivos, A., & Petersen, E. E. (1959). An Experimental Study of Heat Transfer to Nitrogen-Oil Mixtures. *Industrial and Engineering Chemistry, 51*(11), 1369-1372.

Korivi, R. N. K., Bhagwat, S. M., & Ghajar, A. J. (2015). Heat Transfer Measurement and Correlations Assessment for Upward Inclined Gas-Liquid Two Phase Flow. *Proceedings of the 1st Thermal and Fluid Engineering Summer Conference*, New York City, USA, August 9-12.

Martin, B. W., & Sims, G. E. (1971). Forced Convection Heat Transfer to Water with Air Injection in a Rectangular Duct. *I&EC Fundamentals, 14*, 1115–1134.

Oshinowo, O., Betts, R. C., & Charles, M. E. (1984). Heat Transfer in Co-Current Vertical Two-Phase Flow. *Canadian Journal of Chemical Engineering, 62*, 194-198.

Ravipudi, S. R., & Godbold, T. M. (1978). The Effect of Mass Transfer on Heat Transfer Rates for Two-Phase Flow in Vertical Pipe. *Proc. of the 6th International Heat Transfer Conference*, Toronto, Canada.

Rezkallah, K. S., & Sims, G. E. (1987). An Examination of Correlations of Mean Heat Transfer Coefficients in Twophase and Two-Component Flow in Vertical Tubes. *AIChE Symp. Series, 83*, 109-114.

Shah, M. M. (1981). Generalized Prediciton of Heat Transfer During Two-Component Gas-Liquid Flow in Tubes and Other Channels. *AIChE Symp. Series, 77*, 140-151.

Sieder, E. N., & Tate, G. E. (1936). Heat Transfer and Pressure Drop of Liquids in Tubes. *Industrial and Engineering Chemistry, 28*, 1429-1435.

Tang, C. C. (2011). A Study of Heat Transfer in Non-Boiling Two-Phase Gas-Liquid Flow in Pipes for Horizontal, Slightly Inclined, and Vertical Orientations. (Ph.D.), Oklahoma State University, Stillwater, Oklahoma.

Tang, C. C., & Ghajar, A. J. (2007). Validation of a General Heat Transfer Correlation for Non-Boiling Two-Phase Flow with Different Flow Patterns and Pipe Inclination Angles. *Proceedings of the 2005 ASME-JSME Thermal Engineering Heat Transfer Connference*, Vancouver, Canada, July 8-12.

APPENDIX A

UNCERTAINTY ANALYSIS

A method proposed by Kline and McClintock (1953) is utilized for the uncertainty calculations for two phase heat transfer. Sample calculations are presented in Tables 3.1 and 3.2.

Assume, a measurement *R* is a function of several independent variables.

$$R = f(x_1, x_2, x_3 \ldots\ldots\ldots\ldots\ldots x_n) \quad \text{(A.1)}$$

The uncertainty (w_R) of measurement of *R* can be performed by the following formula proposed by Kline and McClintock (1953):

$$w_R = \pm[(\frac{dR}{dx_1}w_1)^2 + (\frac{dR}{dx_2}w_2)^2 + (\frac{dR}{dx_3}w_3)^2 + \quad \ldots\ldots\ldots \quad + (\frac{dR}{dx_n}w_n)^2\ ]^{\frac{1}{2}} \quad \text{(A.2)}$$

According to this method, the uncertainty of the independent variables of heat transfer coefficient equation are first separately calculated and then the individual uncertainties are replaced in the formula to obtain the total uncertainty of heat transfer measurements.

The method of heat transfer uncertainty calculation along with all the equations which are used in every step are described in details as follows:

The heat transfer coefficient equation is given as:

$$h = \frac{\dot{q}''}{\bar{T}_{wi} - \bar{T}_b} = \frac{\dot{q}''}{\Delta T} \tag{A.3}$$

Applying Kline and McClintock (1953) method we can determine the uncertainty for *h*:

$$w_h = \left[\left(\frac{\partial h}{\partial \dot{q}''} w_{\dot{q}''} \right)^2 + \left(\frac{\partial h}{\partial \Delta T} w_{\Delta T} \right)^2 \right]^{\frac{1}{2}} \tag{A.4}$$

After performing the partial differentiation the equation becomes:

$$w_h = \left[\left(\frac{1}{\Delta T} w_{\dot{q}''} \right)^2 + \left(\frac{-\dot{q}''}{\Delta T} w_{\Delta T} \right)^2 \right]^{\frac{1}{2}} \tag{A.5}$$

From Eq. (A.3) it is evident that to determine the uncertainty for *h*, uncertainties associated with $\dot{q}'', \bar{T}_{wi}$ and $\bar{T}_b$ have to be determined. The uncertainty regarding ΔT can be determined by summing up the uncertainties of average inside wall surface temperature and average bulk temperature of the two phase flow.

Now, the average wall inside surface temperature can be expressed with the following equation:

$$\bar{T}_{wi} = \dot{q} R_t + \bar{T}_{wo} \tag{A.6}$$

The uncertainty equation:

$$w_{\bar{T}_{wi}} = \left[\left(\frac{\partial \bar{T}_{wi}}{\partial \dot{q}} w_{\dot{q}} \right)^2 + \left(\frac{\partial \bar{T}_{wi}}{\partial R_t} w_{R_t} \right)^2 + \left(\frac{\partial \bar{T}_{wi}}{\partial \bar{T}_{wo}} w_{\bar{T}_{wo}} \right)^2 \right]^{\frac{1}{2}} \tag{A.7}$$

After simplification the equation becomes:

$$w_{\bar{T}_{wi}} = \left[\left(R_t w_{\dot{q}} \right)^2 + \left(\dot{q} w_{R_t} \right)^2 + \left(w_{\bar{T}_{wo}} \right)^2 \right]^{\frac{1}{2}} \tag{A.8}$$

The experimental set up has seven temperature stations with each station having four thermocouples. The average wall outside surface temperature at each station is determined by

taking the numerical average of the temperature of the four thermocouples using the following equation:

$$\bar{T}_{wosn} = \frac{\bar{T}_{wo-1} + \bar{T}_{wo-2} + \bar{T}_{wo-3} + \bar{T}_{wo-4}}{4} \tag{A.9}$$

Then the average temperature of the seven stations is determined to calculate the average outside wall surface temperature for the whole setup using the following equation:

$$\bar{T}_{wo} = \frac{\bar{T}_{wo-1} + \bar{T}_{wo-2} + \bar{T}_{wo-3} + \bar{T}_{wo-4} + \bar{T}_{wo-5} + \bar{T}_{wo-6} + \bar{T}_{wo-7}}{7} \tag{A.10}$$

The uncertainty associated with each thermocouple temperature is $\pm 0.5^0$C. The outside wall surface temperature has been determined by taking the average at each station; hence, the associated uncertainty with the average wall outside surface temperature is also taken as $\pm 0.5^0$C.

The equation for thermal resistance for the setup is:

$$R_t = \frac{\ln\left(D_o / D_i\right)}{2\pi k l} \tag{A.11}$$

The uncertainty equation is:

$$w_{R_t} = \left[\left(\frac{\partial R_t}{\partial D_o} w_{D_o} \right)^2 + \left(\frac{\partial R_t}{\partial D_i} w_{D_i} \right)^2 + \left(\frac{\partial R_t}{\partial k} w_k \right)^2 + \left(\frac{\partial R_t}{\partial l} w_l \right)^2 \right]^{\frac{1}{2}} \tag{A.12}$$

After substituting the terms we get:

$$w_{R_t} = \left[\left(\frac{1}{2\pi D_o k l} w_{D_o} \right)^2 + \left(\frac{-1}{2\pi D_i k l} w_{D_i} \right)^2 + \left(\frac{-\ln\left(D_o / D_i\right)}{2\pi k^2 l} w_k \right)^2 + \left(\frac{-\ln\left(D_o / D_i\right)}{2\pi l^2 k} w_l \right)^2 \right]^{\frac{1}{2}} \tag{A.13}$$

The uncertainty value for thermal resistance calculated by using Eq. (A. 13) is $\pm$0.51%. It should be noted that the uncertainty for the thermal conductivity value is considered negligible as the value has been determined from best fit curve of tabulated value.

The heat transfer rate has the following equation:

$$\dot{q} = V_D I \tag{A.14}$$

The uncertainty equation becomes:

$$w_{\dot{q}} = \left[\left(\frac{\partial \dot{q}}{\partial V_D} w_{V_D} \right)^2 + \left(\frac{\partial \dot{q}}{\partial I} w_I \right)^2 \right]^{\frac{1}{2}} \tag{A.15}$$

After performing the manipulation we get:

$$w_{\dot{q}} = \left[\left(I w_{V_D} \right)^2 + \left(V_D w_I \right)^2 \right]^{\frac{1}{2}} \tag{A.16}$$

This uncertainty regarding heat transfer rate is calculated by using the equation for heat input from the welder which takes into account the manufacturer recommended uncertainties for the voltage (V_D) and current (I). However, there is also heat loss due to the surroundings from the setup and heat storage in the setup. The amount of heat loss can be calculated from the difference between the heat input rate from the welder and heat transfer rate calculated by using the enthalpy equation to the flow which is:

$$\dot{q} = \dot{m} c (T_{b,out} - T_{b,in}) \tag{A.17}$$

This heat balance error is added with the uncertainty obtained by using Eq. (A.16) to obtain the total uncertainty of heat transfer rate.

The heat flux equation is:

$$\dot{q}'' = \frac{V_D I}{\pi D_i l} \tag{A.18}$$

Hence, the uncertainty equation for heat flux is:

$$w_{\dot{q}''} = \left[\left(\frac{\partial \dot{q}''}{\partial V_D} w_{V_D} \right)^2 + \left(\frac{\partial \dot{q}''}{\partial I} w_I \right)^2 + \left(\frac{\partial \dot{q}''}{\partial D_i} w_{D_i} \right)^2 + \left(\frac{\partial \dot{q}''}{\partial l} w_l \right)^2 \right]^{\frac{1}{2}} \tag{A.19}$$

After substituting the appropriate values, the heat flux uncertainty equation becomes:

$$w_{\dot{q}''} = \left[\left(\frac{I}{\pi D_i l} w_{V_D} \right)^2 + \left(\frac{V_D}{\pi D_i l} w_I \right)^2 + \left(\frac{-V_D I}{\pi D^2{}_i l} w_{D_i} \right)^2 + \left(\frac{-V_D I}{\pi D_i l^2} w_l \right)^2 \right]^{\frac{1}{2}} \tag{A.20}$$

After calculating all the intermediate uncertainty values, they are replaced in Eq. (A.4) to obtain the total uncertainty of the heat transfer coefficient *h*.

VITA

Tarebi Joseph John

Candidate for the Degree of

Master of Science

Thesis: NON-BOILING HEAT TRANSFER IN DOWNWARD INLCINED GAS-LIQUID TWO PHASE FLOW

Major Field: Mechanical and Aerospace Engineering

Biographical: Born and raised in Nigeria.

Education:

Completed the requirements for the Master of Science in Mechanical and Aerospace Engineering at Oklahoma State University, Stillwater, Oklahoma in July 2015.

Completed the requirements for the Bachelor of Science in Mechanical Engineering at Midwestern State University, Wichita Falls, Texas in May 2013.

Experience:

Energy Engineering Intern May 2014-June 2015
Utilities and Energy Management Dept., Oklahoma State University, Stillwater, OK

1) Estimation of the dollar amount of energy loss in the steam pipe system at OSU.
2) Assist in setting up Asset location and Preventative Maintenance system using Asset and Inventory Management Software (AIM) for OSU's Production and Distribution systems.

Manufacturing Engineering Intern Feb. 2012-Jan. 2013
Tranter Heat Transfer Company, Wichita Falls, TX

1) Remodeled work stations to allow for effectiveness and increased productivity by sorting, systemizing, shining, standardizing and sustaining of the work station area.
2) Created standard work instructions for various manufacturing process like plate pressing, assembly of heat exchanger units to help new workers learn the standard work process.